SMOOTH MUSCLE CELL ORGANIZATION IN THE STEM REGION OF THE GRACILIS COLLATERAL CIRCULATION IN BALB/C MICE

A Senior Project

presented to

the Faculty of the Biomedical Engineering Department,

California Polytechnic State University,

San Luis Obispo

In Partial Fulfillment

of the Requirements for the Degree

Bachelor of Science in Biomedical Engineering

By

Laura Lenae Burckhardt

December 2014

PROJECT INFORMATION

TITLE:	Smooth Muscle Cell Organization in the Stem Region of the Gracilis Collateral Circulation in BALB/c Mice
AUTHOR:	Laura Lenae Burckhardt
DATE SUBMITTED:	December 2014
ADVISOR**:**	Trevor R. Cardinal, Ph.D.

ABSTRACT

SMOOTH MUSCLE CELL ORGANIZATION IN THE STEM REGION OF THE GRACILIS COLLATERAL CIRCULATION IN BALB/C MICE

Laura Burckhardt

Of the approximately 8 million Americans who suffer from ischemic peripheral arterial occlusive disease (PAOD), many present with intermittent claudication, or pain associated with exercise. Impaired vasodilation of resistance vessels is a potential explanation for this symptom. Occluded arteries can lead to increased flow through collateral vessels, which function as natural bypasses around the obstruction. This increase in blood flow and resulting shear stress can cause outward remodeling, or arteriogenesis, which improves the efficacy of collaterals. However, following femoral artery ligation in a mouse model of chronic ischemia, vasodilation in the stem region of collateral vessels is impaired at day 7. In the outwardly remodeled collateral stem, the vessel diameter increase is not associated with cell proliferation, suggesting the functionality of the present smooth muscle cells (SMCs) may account for the impaired vasodilation. A potential mechanism for increased vessel diameter in the collateral stem is mechanoadaptation of the vascular SMCs to adapt to the increased fluid shear stress as a result of the increased blood flow. Indeed, decreased SMC overlap and increased SMC length (indicators of mechanoadaptation) coincides with impaired vasodilation in the C57BL/6 mouse strain, which exhibits a large number of collateral vessels and robust collateral remodeling. Collateral density, remodeling following an ischemic event, and VEGF-A expression differ widely among mouse strains, with BALB/c mice exhibiting impaired arteriogenesis due to a polymorphism of the *Vegfa* gene. It is hypothesized that following femoral artery occlusion in BALB/c mice, the SMC mechanoadaptation in the profunda femoris artery will be impaired, which should normalize vasodilation, if mechanoadaptation is a cause of impaired vasodilation in the collateral stem. To test this hypothesis, the femoral artery was ligated in BALB/c mice, before maximal vasodilation at day-7 post-surgery. The animals were then perfusion fixed before resecting and immunostaining the profunda femoris artery to measure SMC length and overlap. The resting and diameters were not different at 40 $\pm$ 3 μm and 48 $\pm$ 2 μm, and the maximally dilated diamters were not different at 61 $\pm$ 4 μm, and 65 $\pm$ 3 μm for the control and day-7 post-ligation profunda femoris arteries, respectively. The increase in diameter for day-7 post-ligation and control profunda femoris arteries were not different, with a percent change of 52 $\pm$ 11% and 41 $\pm$ 3%. SMC length between day-7 post-ligation and control hindlimbs was not different, at 351 $\pm$ 26 μm verses 318 $\pm$ 57 μm in the control. SMC overlap reduced in the day-7 post-ligation hindlimb, 18 $\pm$ 2 μm versus 22$\pm$ 4 μm in the control. These results indicate a subtle impairment in BALB/c collateral stem remodeling, and suggest that the cell processes involved in increasing smooth muscle cell length may impair vasodilation signaling. Further studies are necessary to evaluate the causal relationship between mechanoadaptive remodeling and impaired vasodilation.

ACKNOWLEDGEMENTS

I would first and foremost like to thank Dr. Trevor Cardinal for the honor of his guidance and mentorship through the project. Thank you for the opportunity to learn from you and contribute to such fascinating research.

I would secondly like to thank Amanda Krall for her direct mentorship in the lab. I could not have finished this project successfully without your patience and willingness to help, and I greatly appreciate the time spent with me in instruction.

Thank you to Dr. Lily Laiho for her willingness to train me on the confocal. Thank you for your flexibility and skills as an educator. Without your guidance, the data analysis would not have been possible.

A special thanks to all of the members of the Microcirculation and Vascular Regeneration Lab for their resolute support throughout the project, as you made it all a pleasure to be involved in this specific lab.

Lastly, thank you to my family and friends for their steadfast care and love.

“Be faithful in small things because it is in them that your strength lies.” –Mother Teresa

Table of Contents

INTRODUCTION 1
Peripheral Arterial Occlusive Disease 1
Arteriogenesis 3
Previous Work 4
Specific Aims of Study 6
MATERIALS AND METHODS 8
Animal Husbandry 8
Collateral Enlargement Model 8
Clinical Ambulation Scoring 9
Intravital Microscopy 10
Confocal Microscopy 11
Statistical Analysis 12
RESULTS 13
Clinical Ambulation Scoring 13
Functional Vasodilation in the Ischemic Profunda 14
Mechanoadaptation 16
APPENDIX A: Femoral Artery Ligation Protocol 24
APPENDIX B: Perfusion Fixation Protocol 25
APPENDIX C: ASMA Staining Protocol 26
APPENDIX D: Confocal Protocol 27
APPENDIX E: Raw Images 28

Table of Figures

Figure 1: Peripheral Arterial Occlusive Disease Overview……1
Figure 2: Blood Flow Improvement with Stenting Intervention……3
Figure 3: Smooth Muscle Cell Mechanoadaptation in Rat Arterioles…… 5
Figure 4: Overview of Hindlimb Vascular Flow……9
Figure 5: Murine Strain Comparison of Days to Normal Ambulation……15
Figure 6: Functional Vasodilation in Ischemic Profunda……16
Figure 7: Confocal Microscopy View of Profunda Femoris Smooth Muscle Cells……17
Figure 8: Profunda Femoris Artery Smooth Muscle Cell Length……18
Figure 9: Profunda Femoris Artery Smooth Muscle Cell Overlap……19

INTRODUCTION

Peripheral Arterial Occlusive Disease

Peripheral arterial occlusive disease (PAOD) affects approximately eight million Americans, and has a higher incidence with increased age, high blood pressure, smoking, high cholesterol, and diabetes [1, 2]. Men and woman are equally affected by PAOD, but there is a correlation between African-American ethnicity with increased risk [2]. More common in the lower extremities, PAOD is characterized by the narrowing or blockage of vessels that carry blood throughout the body, typically caused by a buildup of fatty plaque in the arteries, or atherosclerosis, **Figure 1** [3, 4]. This narrowing or blockage can lead to ischemia, or inadequate blood flow to maintain normal tissue metabolic function [5]. Due to this lack of blood supply, the chief symptom of PAOD is intermittent claudication, or pain in the affected region with physical exertion that is alleviated with rest [6, 7]. Patients who present with this symptom often concurrently show impaired

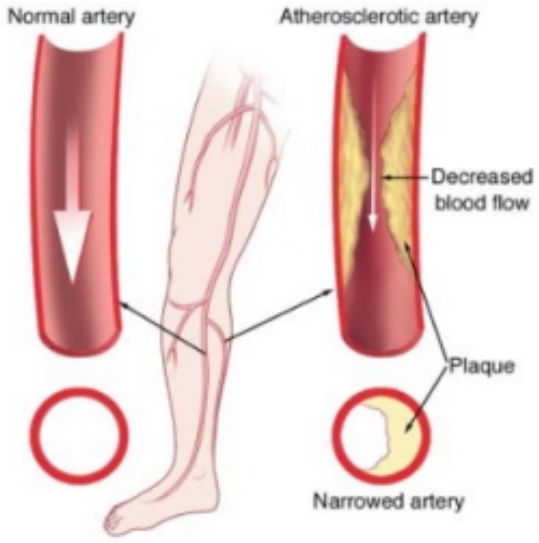

Figure 1: Arterial Occlusive Disease Overview. Comparison of blood flow through a non-atherosclerotic artery verses an atherosclerotic artery [2].

vasodilation, suggesting they also have a reduced ability to regulate blood flow in non-occluded vessels [8]. Vasodilation is critical in supporting standard tissue function by increasing blood flow in response to metabolic needs.

In patients presenting with symptoms of PAOD, there are several tests utilized in diagnosis. The ankle-brachial index compares ankle blood pressure with arm blood pressure, with a low index suggesting artery blockage [9]. Ultrasound tests utilize sound waves to check for blocked or diseased arteries [2]. Magnetic resonance angiography and computed tomographic angiography utilize a contrast dye injected through an IV, in conjunction with a MRI or a CT scan, respectively, to visualize the vasculature and identify areas of concern [7]. Patients with PAOD are at a high risk for developing coronary artery disease and cerebrovascular disease, which are precursors to myocardial infarctions and strokes, respectively [2].

Current treatments for PAOD aim to impede the progression of disease by natural, pharmacologic, or mechanical mechanisms. The first line of therapy is lifestyle changes, such as cessation of smoking, increased exercise regimens, and diet. Post-lifestyle changes or in conjunction with, pharmacologic agents such as aspirin or other anti-platelet medications are prescribed to prevent the development of PAOD-associated complications [6]. For patients in whom these therapies are ineffective, invasive approaches such as balloon angioplasty with stenting **(Figure 2)** or surgical bypass are the next treatment options. Stenting may not be a permanent solution however, as vessels may restenose, or re-narrow around the stent due to intimal hyperplasia [10]. In addition, bypass surgery is a high-risk procedure, and even if successful, may need to be revisited

due to occlusion of the bypass vessel [11]. Due to the sub-optimal performance of current treatment options, alternative therapies are necessary.

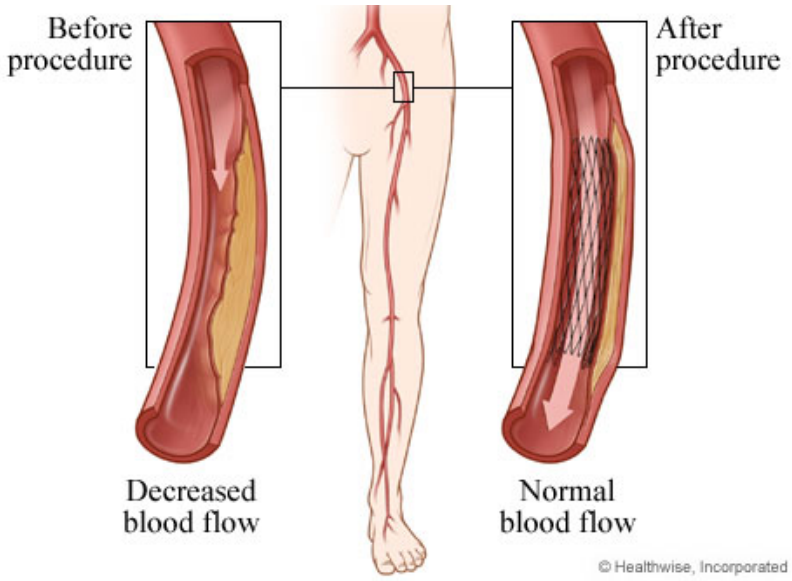

Figure 2: Blood Flow Improvement with Stenting Intervention. Overview of therapeutic option for PAOD, with blood flow returned to normal after stenting [12].

Arteriogenesis

Although bypasses around occlusions can be surgically created, there are natural bypasses that may aid in normalizing blood flow. Initiated by a hemodynamically relevant stenosis of a main feeding artery, blood is redirected through alternative collateral vessels [13]. These vessels act as natural bypasses to the stenosis, connecting a high pressure region to a low-pressure region, thus increasing blood velocity and associated fluid shear stress through the collaterals, improving prognosis due to delivery of oxygen to tissue [13]. A mechanism of the vascular growth, arteriogenesis is the remodeling of preexisting collateral arteries, induced by the increased fluid shear stress

and characterized by a chronically increased luminal diameter that normalizes the fluid shear stress [13, 14].

The initial shear stress of the increased blood flow leads to increased monocyte chemoattractant protein-1 (MCP-1) expression on endothelial cells, and of surface receptors involved in the tethering, rolling, and migration of monocytes. Following extravasation, monocytes transform into macrophages and produce numerous cytokines, growth factors, and enzymes. These agents include matrix-metalloproteinases (MMPs), which degrade the extracellular matrix to allow for outward enlargement of the vessel wall, and tumor necrosis factor-α (TNF-α), which is an inflammatory agent that positively modulates arteriogenesis [15]. VEGF is also secreted, inducing endothelial cell proliferation [16]. There are three regions in the collateral: the stem, midzone, and reentry, with the preceding mechanistic explanation most accurately reflecting arteriogenesis in the midzone. Interestingly, arteriogenesis of the collateral stem may involve either SMC proliferation, as is traditionally described, or mechanoadaptation, which is the rearrangement of the SMCs in order to increase vessel diameter [17,18]. Single factor trials for the stimulation of arteriogenesis, such as the addition of Vascular Endothelial Growth Factor (VEGF) or fibroblast growth factor (FGF), have failed to show therapeutic benefits [19]. Arteriogenesis may still offer a promising therapeutic target, although a holistic understanding of the mechanisms involved is crucial for successful next-generation therapies [13].

Previous Work

SMC mechanoadaptation is characterized by morphological changes in cellular organization and shape [18]. This modification has been investigated in rat arterioles in

response to prolonged exposure of norepinephrine (NE), a vasoconstrictor [18]. Arterioles exposed to NE for 4 hours did not return to original resting diameter upon removal of the NE, due to a significant increase in SMC overlap causing remodeling of the vascular wall and indicating SMC mechanical reorientation **Figure 3** [18]. This phenomenon may occur due to the mechanisms involved in increasing overlap between cells utilizing less energy than cellular constriction.

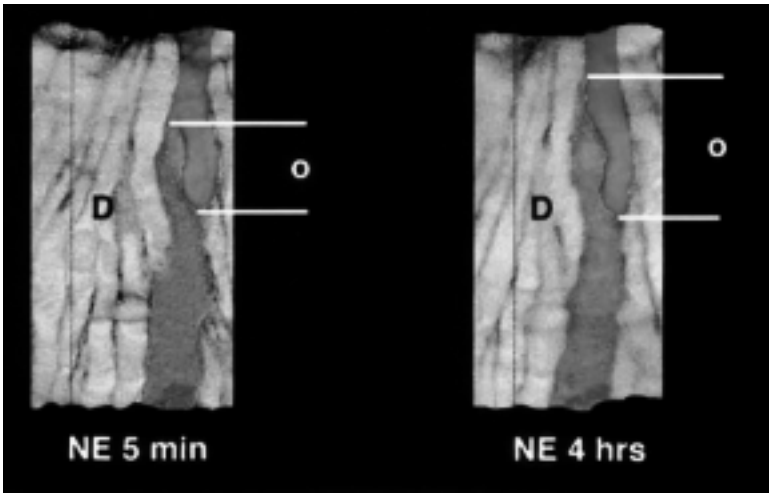

Figure 3: Smooth Muscle Cell Mechanoadaptation in Rat Arterioles. Increase in SMC overlap in rat arterioles when exposed to the vasoconstrictor norepinephrine for prolonged periods of time [18].

The profunda femoris artery, the collateral stem of the gracilis collateral circulation, has an increased resting and maximally dilated diameter on day-7 following creation of a chronic ischemic model via femoral ligation. This increase was associated with an increase in blood flow, as well as endothelial and smooth muscle-dependent vasodilation impairment [20]. As the collateral enlarges, there is a phenotypic change in SMCs from contractile to synthetic, due to the enhanced proliferative nature of the synthetic phenotype. With increased counts of synthetic, non-contractile cells, although SMC numbers increase and the corresponding vessel diameters enlarge, vessel reactivity

would be impaired [21]. However, there was no difference in the number of SMCs in the profunda of the day-7 post-ligation hindlimb verses the control hindlimb, suggesting an alternate factor other than cell proliferation was involved with the observed increased vessel diameter, such as mechanoadaptation [20]. This was supported with observation of an increase in SMC length in the day-7 post-ligation hindlimb of C57BL/6 models, and a decrease in SMC overlap [22].

With this observation applying to C57BL/6 models, it is important to remember that mouse strains differ widely in collateral density and remodeling following ischemic events [23]. Collateral and hindpaw perfusion were lower in BALB/c than C57BL/6, which can be explained by lower collateral density, and BALB/c exhibited greater hindlimb use impairment when compared to the C57BL/6 models. A potential molecular explanation for this impairment is reduced TNF-∝ expression, an inflammatory cytokine that positively modulates arteriogenesis, which was 50% lower in BALB/c mice. Additionally, a cis-acting polymorphism in the *Vegfa* gene in BALB/c could contribute to reduced VEGF-A expression, a growth factor for endothelial cell proliferation, and in turn decreased collateral density and remodeling [23]. These explanations are more associated with the classic arteriogenesis seen in the midzone region, and do not necessarily account for the reorganization of the smooth muscles cells seen in the stem region. Examination of the differences associated with each strain with regards to mechanoadaptation has yet to be shown in literature.

Specific Aims of Study

With a high prevalence of peripheral arterial occlusive disease, and sub-optimal performance of current treatments options, it is clear that alternative therapeutic targets

need to be established. This begins with a greater understanding of the mechanism of collateral enlargement, the process in which preexisting collateral arteries outwardly remodel to form conduit vessels. Following an arterial occlusion, increase in shear stress induces collaterals to increase in diameter and lose functionality in terms of vasodilation. The number of SMCs does not increase, suggesting SMC proliferation is not the cause of outward collateral remodeling. SMC overlap decreases, with longer SMC lengths in C57BL/6 murine models, suggesting mechanoadaptation of the SMCs. Collateral density, remodeling following an ischemic event, and VEGF-A expression differ widely among murine strains, with BALB/c mice showing impaired arteriogenesis potentially due to a cis-acting polymorphism of the *Vegfa* gene. With this information in mind, the aims of this study were to:

1.) Test the hypothesis that a strain of mouse that exhibits impaired mid-zone arteriogenesis will also exhibit impaired mechanoadaptation, by examining SMC length and overlap in the stem region of the gracilis collateral circulation
2.) Test the hypothesis that mechanoadaptation impairs vasodilation, by observing if an inhibited degree of mechanoadaptation results in normalized vasodilation in response to vasodilatory agents SNP and papaverine

MATERIALS AND METHODS

Animal Husbandry

Male BALB/c mice were used for all experimental procedures according to the protocols approved by the Institutional Care and Use Committee (IACUC) of California Polytechnic State University (Cal Poly). All mice were maintained in a temperature and 12-hour light cycle controlled room in the University Vivarium. Mice were specifically housed by litter in micro-isolator cages, supplied with feed, water, and enrichment (houses and tubes), and monitored daily.

Collateral Enlargement Model

A murine collateral enlargement model was created via femoral artery ligation in the left hindlimb of the animals. Prior to surgery, the surgical bench was disinfected with 70% isopropyl alcohol, and all surgical instruments and materials were sterilized in an autoclave. After weighing the animal, mice were anesthetized using 1-3% isoflourane gas at an oxygen flow rate between 0.8-1.2 $l \cdot min^{-1}$, administered through a nose-cone. Hair on the anterior hindlimb was depilated, and surgical area was disinfected with Nolvasan. The mice were placed in a supine position on a controlled heated surgical stage, with a rectal probe monitoring the animal's core-body temperature. Veterinary ointment was added to the eyes to avoid corneal desiccation.

A small incision was made on the middle, medial aspect of the left thigh, which was then extended to the abdominal wall. The subcutaneous connective tissue was blunt dissected to maximize surgical exposure. Throughout the procedure, the incision site was irrigated with sterile phosphate buffered saline (PBS) to prevent tissue desiccation. To expose the ligation site, the epigastric fat pad was reflected medially following blunt

dissection. The femoral artery was blunt dissected from the neurovascular bundle downstream from the deep femoral branch. The femoral artery was ligated with 6.0 silk suture distal to the epigastric branch and proximal to the popliteal branch, **Figure 4**. The skin was closed using 7.0 polypropylene suture. For control, the surgical procedure outlined previously was performed on the contralateral hindlimb, with the exception of the ligation of the femoral artery. Post-surgery, animals were given a subcutaneous injection of buprenorphine (0.075mg/kg), and supplied with buprenorphine water (0.01 mg/mL) for 2-3 days.

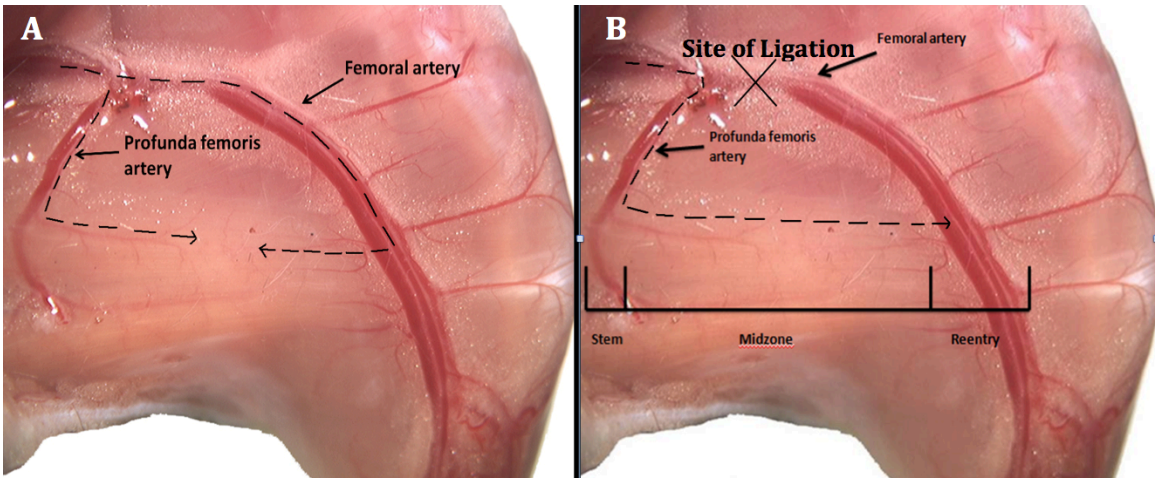

Figure 4. Overview of Hindlimb Vascular Flow. A) Normal blood flow through hindlimb, directionally indicated though dotted lines and arrows. B) Indicated site of ligation with resulting redirection of blood flow through the profunda femoris artery and collateral [21].

Clinical Ambulation Scoring

Following the surgery, animals were observed daily for ambulation, and scored from 0-3 based on hindpaw range of motion. A dragging hindpaw established a score of 3, no plantar flexion and constant dorsiflexion constituted a score of 2, some planar flexion a 1, and normal use a 0. Animals were monitored until normal ambulation was observed on two consecutive days, or until day-7 post-ligation.

Intravital Microscopy

To analyze the vasodilatory capacity of the collateral stem, vasodilation was assessed in mice 7-days post-ligation. The surgical area was prepared and mice were anesthetized as described previously. A small incision was made on the middle, medial aspect of the left hindlimb, with the incision continued up the abdominal wall. The subcutaneous connective tissue was blunt dissected to maximize surgical exposure, the epigastric artery vein pair was cauterized and the epigastric fat pad was removed. The skin overlying the saphenous artery-vein pair and profunda femoris artery-vein pair was removed to maximize exposure and improve visibility. PBS was dripped over exposed tissue, and plastic wrap was placed over area to prevent desiccation, before a 30–minute equilibration period before vasodilator application, during which time the contralateral limb was exposed.

An intravital microscope, the Olympus BXFM, with a 5x objective and interface with QCapture imaging software was utilized to capture images of the profunda femoris artery at rest and following maximal vasodilation. This dilation was in response to sodium nitroprusside (SNP, 10^{-3}) and papaverine (10^{-2}), which were applied for 5 minutes prior to imaging. This procedure was repeated on the contralateral side.

Sample Perfusion and Fixation

In order to ensure cylindrical vascular dimensions were preserved post-resection, mice were perfusion fixed. Through a thoracotomy, an incision was made in the apex in the heart into the left ventricle, and a catheter was inserted and secured with a vascular clamp. A cycle of 10mL PBS, then 5mL 4% paraformaldehyde (PFA), followed by 10ml PBS was driven through the catheter, with a syringe pump (4 mL/min). During this cycle,

SNP and papaverine were applied to the superficial areas of the hindlimb, to ensure that the maximum diameter of the profunda femoris was maintained. Post fixation, the anterior gracilis muscle and profunda femoris artery were resected and post-fixed in 4% PFA for approximately 24 hours before being rinsing and storing in PBS at 4°C.

Confocal Microscopy

Confocal microscopy was used to visualize smooth muscle cells around each artery. Samples were stained with 1:200 1A4 clone (α-smooth muscle actin, Cy3 conjugate) with 0.1% saponin and 2% BSA reconstituted in PBS for 7 days, with 0.3 mL of solution per sample. Following, they were washed in 0.1% saponin in PBS 3x for 20 minutes at room temperature, and then in PBS for 30 minutes. The samples were then mounted onto depression slides with 50/50 PBS and Glycerol. Utilizing a confocal microscope and 40x oil immersion objective, images of the profunda femoris artery were captured with Fluoview Viewer (FV10-ASW 4.1) software. Image stacks in the z direction were taken with 1-micron slices to approximately half the diameter for each artery.

Image Analysis

The intravital microscopy images of the profunda femoris at rest and maximum dilation were used to measure average diameter of the vessel at those two conditions. The z-stacks of the profunda femoris, taken with the confocal microscope, were merged into single, 3-D reconstructions. These images were used to measure average smooth muscle cell overlap between the individual cells, determined by measuring all of the distinguishable overlaps between cells on the image, and averaging those values. In addition, smooth muscle cell length measurements were determined based on a formula

validated in previous studies [18, 24], utilizing statistical patterns of SMC orientation to establish average SMC lengths with a single view of the image. This formula requires several assumptions, as follows:

1. The vessels studied are fully dilated and cylindrical in shape.
2. There is only one layer of SMCs surrounding the studied vessel.
3. The SMCs have 2 end points only.
4. There are only two visible types of cells: "wrap cells, extending across the entire visible portion of the vessel, and "taper" cells, partially extending the visible portion of the vessel.

A 100μm length of artery was delineated for each 3D reconstruction, and average SMC length for each vessel, L_v, was determined using Equation 1 below [18, 24]:

$$L_v = 4\pi R_v F(S_w + S_t)/T_v \quad \text{(Eq. 1)}$$

In equation 1, L_c is the average SMC length, R_v is the radius of the artery, F is the fraction of vessel circumference in which measurements were made, S_w is the number of wrap cells, S_t is the length of all tapered cells divided by the length of one wrap cell, and T_v is the number of taper cells.

Statistical Analysis

Independent Student's t-tests were performed between the data from control and day-7 post-ligation hindlimbs, as well as the ambulation data between mice strains. A p-value of less than 0.05 indicated statistical significance.

RESULTS

The aims of this study were to test the hypothesis of smooth muscle cell mechanoadaptation impairment in BALB/c mice during outward remodeling of the collateral stem following an ischemic event, as well as examine if impaired mechanoadaptation normalized vasodilation. The first objective within these aims was to investigate functional hindlimb use impairment when compared to C57BL/6 mice, which possess well-developed collaterals, as quantified by clinical ambulation scoring. The second objective was to measure the resting and maximally-dilated profunda femoris artery *in vivo* to test if collateral enlargement occurred, along with impaired vasodilation 7 days post-ischemic event. The third objective was to test the hypothesis of mechanoadaptation by determining SMC overlap and length in the profunda.

Clinical Ambulation Scoring

It was expected that BALB/c mice would have greater functional hindlimb impairment when compared to C57BL/6 mice [22]. The recovery time to normal hindlimb ambulation trended towards longer in BALB/c mice, with 6 ± 0.4 days, where C57BL/6 mice required 5 ± 0.3 days, **Figure 5.**

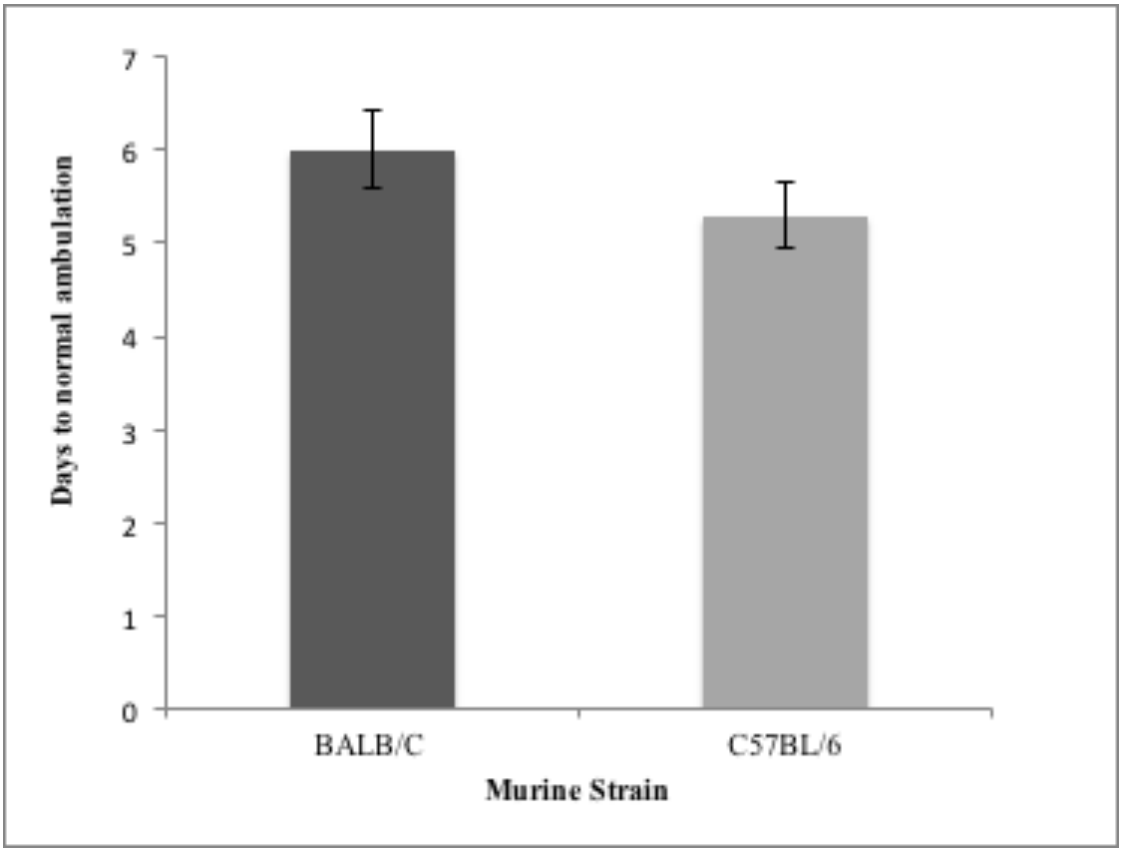

Figure 5: Murine Strain Comparison of Days to Normal Ambulation. Average days to return to normal hindlimb use following ischemic event, as determined by clinical ambulation scoring.

Functional Vasodilation in the Ischemic Profunda

As poor ambulation results are suggestive of functional impairment, this was next examined. Both resting and maximally dilated diameters of the profunda femoris artery on the day-7 post-ligation limbs trended towards greater diameters than the control hindlimb, although the results were not statistically significant ($p > 0.05$). The resting diameters were 40 ± 3 μm and 48 ± 2 μm, and the maximally dilated diameters were 61 ± 4 μm 65 ± 3 μm for the control and day-7 post-ligation hindlimbs, respectively. The increase in diameter for day-7 post-ligation and control limbs were not different, and represented a percent change of $52 \pm 11\%$ and $41 \pm 3\%$, respectively (**Figure 6**).

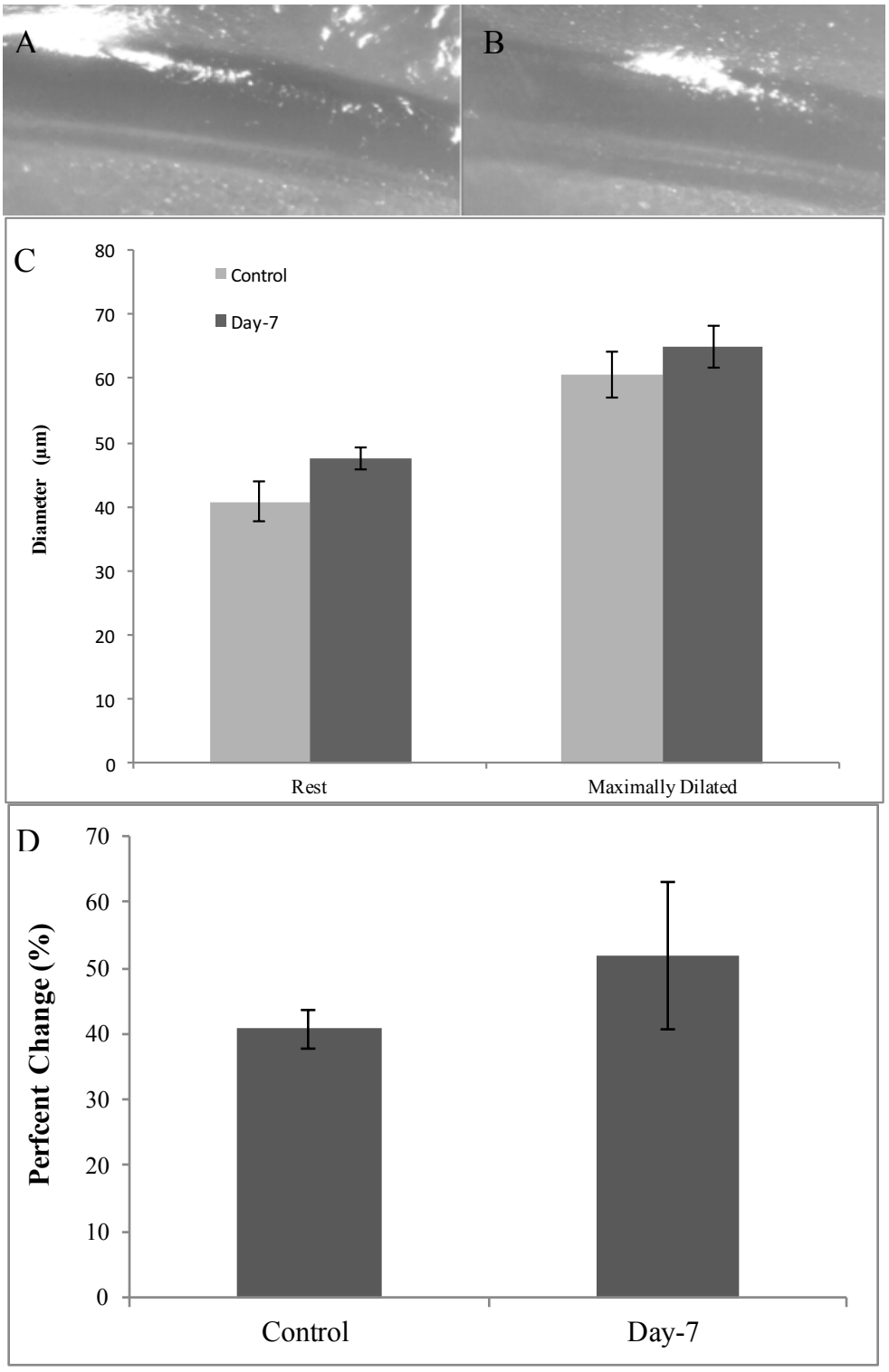

Figure 6: Functional Vasodilation in Ischemic Profunda. A) Representative images of profunda femoris at resting diameter and B) at maximally dilated diameter in response to papaverine and SNP C) Average vessel diameter resting and maximally dilated diameters for control and day-7 post-ligation hindlimbs. D) Percent change in vessel diameter from resting to maximum dilation, n=7.

Mechanoadaptation

The absence of impaired vasodilation is suggestive of a lack of remodeling, so indicators of mechanoadaptation, SMC length and overlap, were examined. The smooth muscle cells trended towards longer lengths in the day-7 post-ligation hindlimb compared to the control hindlimb, although the results were not significant ($p>0.05$), with the lengths in the control hindlimb of 318 ± 57 μm, and in the day-7 post-ligation hindlimb of 351 ± 26 μm. An overview of the types of SMCs, wrap and taper, which were used to calculate SMC lengths can be seen in **Figure 7**, with the results in **Figure 8**.

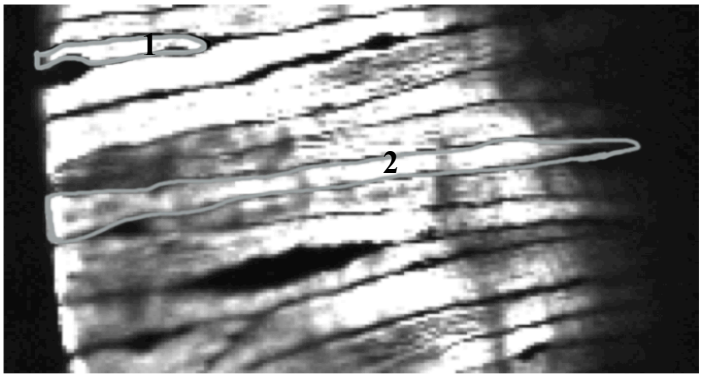

Figure 7: Confocal Microscopy View of Profunda Femoris Smooth Muscle Cells. 1) Taper cell partially extends across visible artery portion. 2) Wrap cell extends across entire visible portion of artery

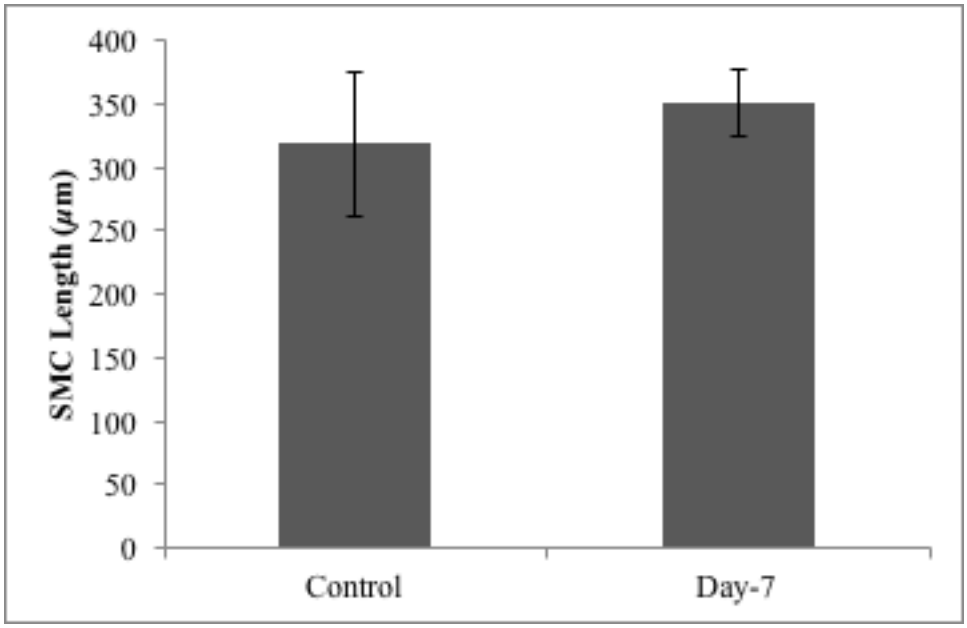

Figure 8: Profunda Femoris Artery Smooth Muscle Cell Length. Average SMC lengths in profunda femoris artery of control and day-7 post-ligation hindlimbs, n=5 control, n=6 day-7.

The average SMC overlap in the control hindlimb was longer than the SMC overlap in the day-7 post-ligation hindlimb, at 22 $\pm$ 4 μm in the control hindlimb and 18 $\pm$ 2 μm in the day-7 post-ligation hindlimb, $p<0.05$.

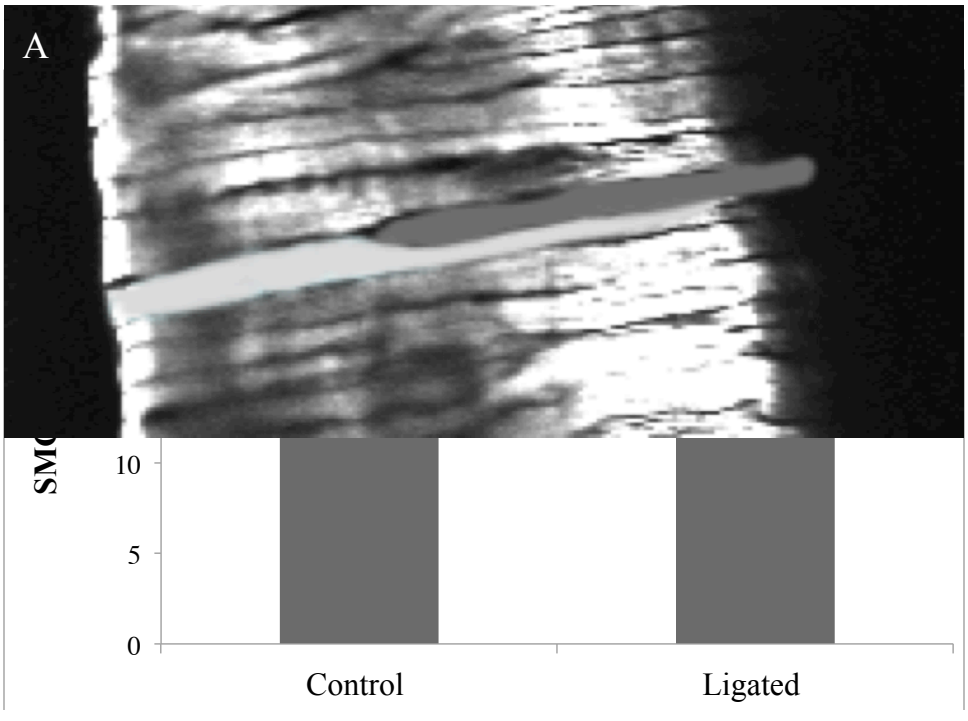

B

Figure 9: Profunda Femoris Artery Smooth Muscle Cell Overlap. A) Example of overlap between two SMCs using confocal microscopy at 40x. B) Average SMC overlap in the profunda femoris artery in the control and day-7 post-ligation hindlimbs, n=5 control, n=6 day-7; $p<0.05$.

Control Day-7

DISCUSSION

Patients who suffer from peripheral arterial occlusive disease may experience intermittent claudication, which may be explained by impaired vasodilation. Therefore, restoring normal vasodilation may reduce associated symptoms, and improve patient prognosis. In mouse models with robust collateral networks and collateral growth, impaired vasodilation can be explained by smooth muscle cell dysfunction, presumably as a result of mechanoadaptation (increased SMC length and decreased SMC overlap) in the context of collateral enlargement. Therefore, we sought to support the causal role of mechanoadaptation in impaired vasodilation by evaluating the degree of mechanoadaptation in an animal model that exhibits reduced arteriogenesis, and the associated vasodilation.

The first objective of the study was to test the hypothesis that an animal model that exhibits reduced arteriogenesis results in decreased functional use following an ischemic event, by examining functional hindlimb use post-femoral artery ligation in comparison to the C57BL/6. This examination allows for calibration of the work to other relative investigative groups, as ambulation scoring is a common assessment. The average amount of days to normal ambulation trended towards higher in BALB/c compared to C57BL/6. This trend was consistent with previous studies, but significance was not observed. As BALB/c exhibit fewer pre-existing collaterals and decreased collateral remodeling, the lack of significance may be due to subjectivity of ambulation scoring, and the resulting inconsistency between the score assigners.

As ambulation scoring only assesses overall functional use of the hindlimb, the second more specific aim of the study investigated functional vasodilation in the ischemic

profunda. Both resting and maximally dilated average diameters of the profunda femoris trended towards greater than the control hindlimb, suggesting arteriogenesis characterized by outward remodeling had ensued, although the results were not significant. The percent change in diameter from resting to maximum dilation was not different in the control and day-7 post-ligation hindlimbs, suggesting vasodilation was not impaired. If mechanoadaptation is impaired within BALB/c mice, this finding is consistent with the hypothesis that mechanoadaption impairs vasodilation.

With normal vasodilation observed in the samples, the final aim of the study was to examine the presence and degree of mechanoadaptation in the ischemic hindlimb, characterized by a decrease in SMC overlap and an increased length. There was not an increase in SMC length in the day-7 post-ligation hindlimb compared to the control hindlimb, but there was a decrease in SMC overlap. This suggests a subtle form of mechanoadaptation in the SMCs of the collateral stem of the ischemic profunda, but an impairment in the degree of remodeling as compared to the C57BL/6 model, potentially due to lower amounts of TNF-∝ and VEGF-A comparatively seen in this strain [23]. It would be interesting to examine whether the presence of these two factors would enhance SMC mechanoadaptation in the BALB/c, which could offer further clarity into a potential therapeutic target. To establish a necessary and sufficient relationship, TNF-∝ and VEGF-A could be inhibited in separate experiments, and the degree of mechanoadaptation in the stem region of the profunda femoris observed.

There were several limitations in this study that may have contributed to variability in the results. In the formula for SMC length, several assumptions were made. One assumption was that the vessels were fully dilated and cylindrical in shape, which is

not entirely feasible even with the precautions of perfusion fixation and the utilization of a depression slide for imaging. Furthermore, it was assumed that there is only one layer of SMCs on the vessel, which was not verified. In the comparison of results from the BALB/c to the C57BL/6 models, the data was compared from two different surgeons. Differences in technique may have led to variation in the data in which a comparison was not appropriate.

Overall, there is a promising correlation between impaired vasodilation and mechanoadaption in varying murine strains. The effect of factors that differ in mice strains such as VEGF-A expression, TNF-∝ levels, and pre-existing collaterals on impaired mechanoadaptation need to be established. With further study, the potential correlation between mechanoadaptation and impaired vasodilation can be prospectively utilized to establish a causal relationship to help better understand impaired vasodilation and other factors involving peripheral arterial occlusive disease. A better understanding of these relationships will hopefully lead to establishing an effective target for future therapeutics.

REFERENCES

1. Roger VL, Go AS, Lloyd-Jones DM, et. al. Heart Disease and Stroke Statistics 2011 Update: A Report from the American Heart Association. *Circulation* 2011;123:e18-e209.
2. "Peripheral Arterial Disease (PAD) Fact Sheet." *Centers for Disease Control and Prevention.* Centers for Disease Control and Prevention, 26 July 2013. Web.
3. Creager MA, Loscalzo J. Vascular Diseases of the Extremities. In: Fauci AS, Braunwald E, Kasper DL, et al., eds. Harrison's Principles of Internal Medicine. 17e ed. New York: McGraw Hill, 2008.
4. Rooke TW, Wennberg PW. Diagnosis and Management of Diseases of the Peripheral Arteries and Veins. In: Walsh RA, Simon DI, Hoit BD, et al., eds.: Hurst's The Heart. 12e ed. New York: McGraw Hill, 2007.
5. "About Peripheral Artery Disease (PAD)." *About Peripheral Artery Diesase (PAD).*
6. Rowe VL. "Peripheral Arterial Occlusive Disease." Medscape. Diagnosis and Management of Peripheral Arterial Disease: A National Clinical Guideline. Edinburgh: Scottish Intercollegiate Guidelines Network, 2006. Print.
7. Poredos P., Golob M., Jensterle M. (2003). Interrelationship between peripheral arterial occlusive disease, carotid atherosclerosis and flow mediated dilation of the brachial artery. Int. Angiol. 22, 83–87
8. Kiani S, Aasen J, Holbrook M, Khemka A, Sharmeen F, LeLeiko R, Tabit C, Farber A, Eberhardt R, Gokce N, Vita J, Hamburg N. Peripheral artery disease is associated with severe impairment of vascular function. *Vascular Medicine* 18: 7278, 2013.
9. "Ankle-brachial Index." - Mayo Clinic. N.p., n.d. Web. 28 Oct. 2015. <http://www.mayoclinic.org/tests-procedures/ankle-brachial-index/basics/definition/prc-20014625>.
10. Dangas, G. "Restenosis: Repeat Narrowing of a Coronary Artery: Prevention and Treatment." Circulation 105.22 (2002): 2586-587. Web.
11. "Peripheral Artery Bypass - Leg: MedlinePlus Medical Encyclopedia." U.S National Library of Medicine. U.S. National Library of Medicine, n.d. Web. 04 Dec. 2014. <http://www.nlm.nih.gov/medlineplus/ency/article/007394.htm>.
12. Healthwise. Web. <http://edu.cardiologyconsultantspa.com/ItemPopup.aspx?HWID=zm6211&SEC=zm6211-sec>.
13. Royen, N. Van. "Stimulation of Arteriogenesis; a New Concept for the Treatment of Arterial Occlusive Disease." Cardiovascular Research 49.3 (2001): 543-53. Web.
14. Buschmann, I., and W. Schaper. "Arteriogenesis Verses Angiogenesis: Two Mechanisms of Vessel Growth." Physiology 14.3 (1999): 121-25. Web.
15. Heil, M., Inka Eitenmüller, T. Schmitz-Rixen, and W. Schaper. "Arteriogenesis versus Angiogenesis: Similarities and Differences." Journal of Cellular and Molecular Medicine 10.1 (2006): 45-55. Web.

16. Fung E, Helisch A. Macrophages in collateral arteriogenesis. *Frontiers in physiology.* 2012; 3:353.
17. Helisch A., Schaper W. Arteriogenesis The Development and Growth of Collateral Arteries. *Microcirculation.* 2003; 10:8397.
18. Martinex-Lemus L, Hill M, Bolz S, Pohl U, Meininger G. Acute mechanoadaptation of vascular smooth muscle cells in response to continuous arteriolar vasoconstriction: implications for functional remodeling. *The FASEB Journal.* 2004.
19. Degen, Achim, Dominic Millenaar, and Stephan Schirmer. "Therapeutic Approaches in the Stimulation of the Coronary Collateral Circulation."CCR Current Cardiology Reviews 10.1 (2014): 65-72. Web.
20. Cardinal T, Struthers K, Kesler T, Yocum M, Kurjiaka D, Hoying J. Chronic hindlimb ischemia impairs functional vasodilation and vascular reactivity in mouse feed arteries. *Frontiers in physiology.* 2011; 2:91.
21. Bynum, A. Cardinal, T. Impact of Collateral Enlargement on Smooth Muscle Phenotype. California Polytechnic State University. December 2011.
22. Krall A. Smooth Muscle Cell Organization in the stem region of the gracilis collateral circulation. Senior project, California Polytechnic State University San Luis Obispo, 2014. DigitalCommons@Calpoly. Web.
23. Chalothorn, D., J. A. Clayton, H. Zhang, D. Pomp, and J. E. Faber. "Collateral Density, Remodeling, and VEGF-A Expression Differ Widely between Mouse Strains." *Physiological Genomics* 30.2 (2007): 179-91. Web.
24. Miller B, Gattone V, Overhage J, Bohlen H, Evan A. Morphological evaluation of vascular smooth muscle cell: Length and width from a single scanning electron micrograph of microvessels. *The Anatomical Record.* 1986; 216:95-103.

APPENDIX A: Femoral Artery Ligation Protocol

Date _____ **Hindlimb Ischemia Surgery - Ligation** Initials _____

Mouse Information
DOB: _____
Sex: _____
Tag: _____
Genotype/strain: _____
Cage: _____

Materials
Sterilize- autoclave or flash autoclave
____1. forceps (2)
____2. fine forceps (2)
____3. ultrafine forceps (1)
____4. fine scissors (1)
____5. microscissors spring loaded (1)

Pre-sterilize in autoclave
____6. cotton gauze (2)
____7. cotton swabs (12)
____8. 6.0 silk suture (2 x 1-inch)
____9. needle holder (1)

Obtained in surgery suite
____10. sterile Petri dish w/ sterile saline
____11. sterile gloves
____12. sterile 7.0 prolene suture
____13. heat-cautery
____14. FST heat pad w/ rectal probe
____15. heat pad
____16. recovery bin & weigh boat
____17. depilatory cream
____18. non-sterile cotton swabs
____19. non-sterile cotton gauze
____20. isolation mask & cap
____21. analgesic (Buprenorphine)

Surgery preparation
____22. Spray surgery area with Nolvasan
____23. Weigh animal in weight boat
____24. Place animal in anesthesia box
____25. Open the oxygen cylinder and set anesthesia-machine flow meter to ~3 $l \cdot min^{-1}$
____26. Anesthetize animal w/ 5% isoflurane
____27. Affix non-rebreathing circuit to bench-top with tape
____28. Reduce flow rate to 0.5-1.0 $l \cdot min^{-1}$ and the isoflurane to 1-3%
____29. Apply ear tag high on left ear
____30. Lay animal supine with nose in nose-cone
____31. Shave hair on the right hindlimb & lower abdomen with clippers
____32. Remove excess hair with depilatory cream
____33. Spray right hindlimb with Nolvasan
____34. Return animal to anesthesia box
____35. Apply 4x4 gauze sponge to heat pad to protect animal from excessive heat
____36. Affix non-rebreathing circuit to surgery table w/ chemistry clamp
____37. Lay animal supine on circulating heat pad w/ nose in nose-cone
____38. Insert rectal probe and set thermo-controller to 37°C
____39. Apply veterinary ointment to eyes to avoid drying during procedure
____40. Apply veterinary ointment to anus and place rectal probe ~1cm into anus to monitor core-body temperature

Surgery
____41. Make a small incision on the middle, medial aspect of the left thigh
____42. Extend the incision up to the abdominal wall
____43. Blunt dissect the subcutaneous connective tissue to maximize surgical exposure
____44. Use cautery to remove fat pad overlying femoral a-v pair & cauterize epigastric av-pair
____45. Blunt dissect the femoral artery from the neurovascular bundle just downstream from the deep femoral branch
____46. Tie off the femoral artery & vein with 6.0 silk suture, just downstream to the deep femoral branch
____47. Use 6.0 polypropylene suture to close the skin
____48. Make a small incision on the middle, medial aspect of the right thing
____49. Extend the incision up to the abdominal wall
____50. Blunt dissect the subcutaneous connective tissue to maximize surgical exposure
____51. Use 6.0 polypropylene suture to close the skin

Post-Surgical
____52. Give the animal an subcutaneous injection of buprenorphine (0.075mg/kg)
____53. Place the animal in the recovery bin, on a blue bench cover, above a heat pad and allow to recover
____54. Turn flow meter down to 0, turn off isoflurane, and close the oxygen cylinder
____55. Indicate surgery on cage card

Notes
_____
_____
_____
_____

APPENDIX B: Perfusion Fixation Protocol

Date _____ **Perfusion Fixation** Initials _____

Mouse Information
DOB: _____
Sex:_____
Tag:_____
Genotype/strain: _____
Cage:_____
Weight(g): _____

Materials
Non-Sterilize Dissection Instruments
____1. forceps (2)
____2. fine forceps (2)
____3. Bone Scissors(1)
____4. Skin Scissors (1)
____5. Dissection Scissors (1)
____6. Hemostats(1)
____7. Vascular clamp (1)

Obtained in surgery suite
____8. Tape
____9. 10mL Syringes (2)
____10. Bench cover
____11. Heating pad
____12. Catheter
____13. Avertin Anesthetic
____14. Non-sterile saline
____15. Cotton swab

Vasodilator Cocktail Preparation
____16. Turn on water bath to 37°C
____17. 400 µL heparin
____18. 1mL SNP(orange)
____19. 600µL Adenosine(clear)
____20. 38mL PBS solution
____21. Thaw SNP and Adenosine
____22. Add heparin, SNP, Adenosine, and PBS solution together in a 50mL conical
____23. Place vasodilator cocktail in water bath
____24. Prepare 15mL of histochoice in a 50mL conical and place in water bath

Procedure Preparation
____25. Weigh animal and draw up appropriate dose of Avertin anesthetic (.15mL/10g)
____26. Obtain saline filled beaker, cotton swab, and instruments

Fixation
____27. Anesthize mouse with Avertin
____28. Heat up heat pad in microwave and wrap with bench cover when warm
____29. Remove hindlimb hair on both legs by shaving
____30. Tape animal down to heated bench cover
____31. Separate skin from muscle from the abdomen to the top of the thoracic cavity
____32. Fill 10mL syringe with warm Vaso D
____33. Cut through abomen close to diaphragm
____34. Quickly cut through the ribs and diaphragm to open chest cavity and clamp back with hemostats
____35. Cut away excess tissue around the heart
____36. Make a small incision in the apex of the heart
____37. Insert catheter and clamp with vascular clamp and cut right ventricle
____38. Inject Vaso D solution into animal approximately 20mL
____39. Inject 12mL of histochoice
____40. Dissect the calf and thigh muscle preserve in histochoice

Notes
_____
_____
_____
_____
_____
_____

APPENDIX C: ASMA Staining Protocol

Materials

24-well culture plates (Cat#: 3738, Corning Incorporated)
PBS
0.1% Saponin (Cat#: 47036, Sigma-Aldrich)
2% Bovine Serum Albumin (Cat# B6917, Sigma Aldrich)
Monoclonal Anti-Alpha Smooth Muscle Actin, Cy3 Conjugate (Cat#: C6198, Sigma-Aldrich)
Slides
Coverslips
Parafilm
Aluminum foil

Staining

1. Using forceps, remove muscle from PBS (stored in microcentrifuge tube at 4°C) and place in a single well of a 24-well culture plate.
2. Prepare antibody solution containing 1:200 1A4 clone (alpha-smooth muscle actin, Cy3 conjugate) in 0.1% saponin (reconstituted in PBS), 2% BSA (reconstituted in PBS) in PBS, using 0.3mL of solution per muscle.
3. Incubate muscle in antibody solution for 3 nights (72 hours) at 4°C). (**Note: Critical step—3 nights crucial for bright staining) by gently pipetting solution over muscle.)**
4. Wash in 0.1% saponin in PBS 3x for 20 minutes at room temperature. Cover plate with foil during each wash.
5. Wash in plain PBS for 30 minutes. Cover with foil during each wash.
6. Place 1-2 drops of 50/50 PBS and Glycerol onto slide.
7. Remove muscle from well using forceps and place on a slide.
8. Add 1-2 drops of 50/50 PBS and Glycerol to the top of the muscle and place cover slips over the muscle.
9. Paint edges of coverslip with clear nail polish to create a seal and prevent tissue desiccation.
10. Store slides at 4°C wrapped in foil or an opaque container between imaging.

Imaging

11. Image using a standard fluorescent microscope. (Cy3 excitation: 550 nm, emission: 570 nm)

APPENDIX D: Confocal Protocol

Date _____ **Confocal Imaging** Initials _____

Materials

___1. Depression slide
___2. Coverglass (.08-.13mm thick)
___3. Clear nail polish
___4. 50/50 PBS-glycerol
___5. Slide box
___6. Forceps (1)

Slide Preparation

___7. Using forceps, gently place the sample into the well on the depression slide with the anterior of the sample facing up
___8. Drop 50/50 glycerol onto the sample
___9. Place coverglass on top of sample and use nail polish to seal the edges

Confocal Microscope Setup and Imaging

___10. Turn on the confocal microscope by switching the seven power buttons starting from top to bottom going from left to right (at the one with the keys, wait for the steady green light to move on)
___11. Log into the log book
___12. Log on to computer: password: fluoview
___13. Open Fluoview Program
___14. Choose "Load Acquisition" to pull up parameters of an old file
___15. Place a single drop of oil onto the 40x objective (this will be the viewing objective)
___16. Turn off the light before removing sample from slide box
___17. Place the sample onto the stage with the coverslip facing downward, toward the objective
___18. Carefully bring the objective closer to the sample using the coarse adjustment until the slide contacts the oil
___19. Open the shutter on the tube as well as the stage to let the fluorescent light in
___20. Turn on the fluorescent light via the icon on the program that has a diamond on top of a circle
___21. Locate the desired location of the vessel for imaging through the eye piece using the coarse and fine objective adjustments located on the bottom of the microscope near to the left and right of the stage
___22. Press XY Repeat on Fluoview program to bring image onto computer
___23. Adjust the power (do not increase the power above 20) to see the clearest image of the sample, making sure that image is not saturated
___24. Find the top of the vessel by altering the Z-plane, moving the fine adjustment clockwise to move to the surface of the sample and counterclockwise to go deeper into the sample
___25. Once the top is determined, click the "Set" button on the bottom left of the program
___26. Next find the end of the Z-stack desired by going deeper into the vessel and set this as the end point
___27. Set the step size to 1µm
___28. Click the Z-stack "XYZ" button to take the Z-stack
___29. Save the file as an .oib onto the computer and export it as a .tiff

Microscope Clean Up

___30. Turn off the microscope in the opposite way it was turned on, from right to left, bottom to top
___31. Make sure to close the shutters
___32. Log out in the log book
___33. Fold a lens sheet and drip isopropyl alcohol (IPA) onto it then make a single swipe over the objective to clean the oil from it, repeat until the lens is clear using several lens sheets, use a cotton tip applicator with IPA to clean the area around the lens on the objective
___34. Cover confocal microscope

Notes

_____
_____
_____

APPENDIX E: Raw Images

In vivo imaging (5x)

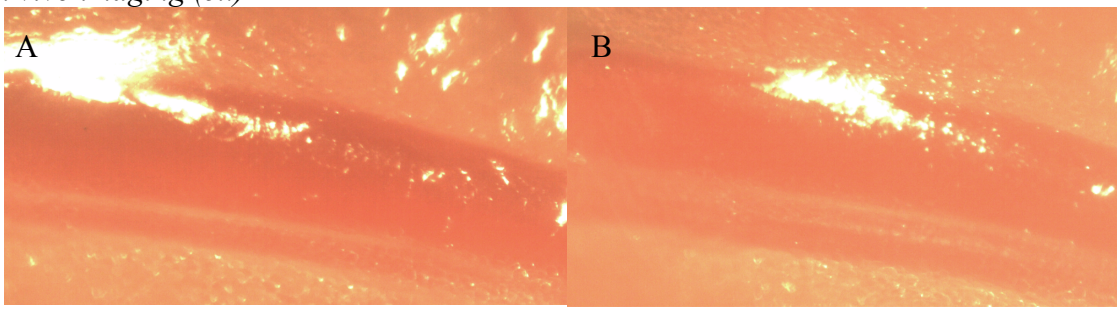

N=1 Profunda Femoris Artery Day-7 Post-Ligation A) Resting B) Maximally Dilated

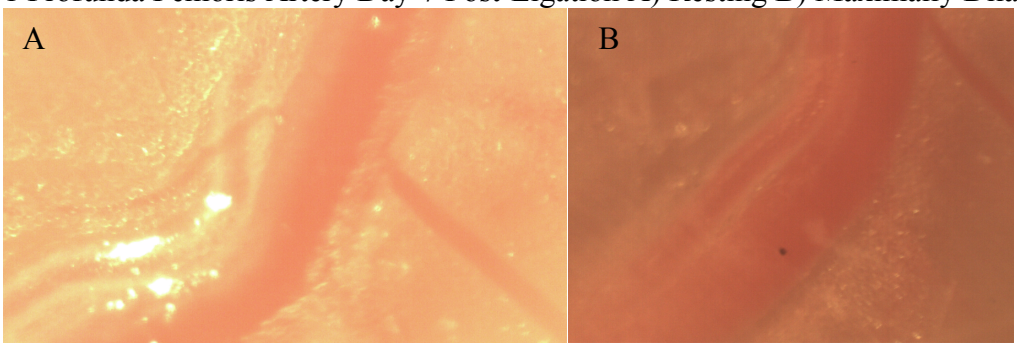

N=1 Profunda Femoris Artery Control A) Resting B) Maximally Dilated

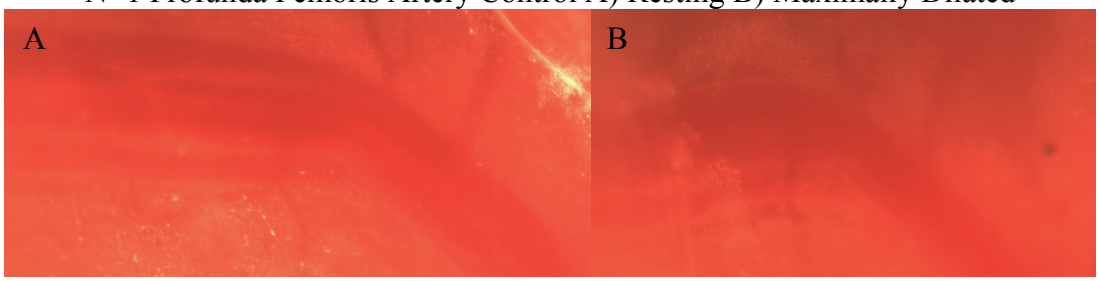

N=2 Profunda Femoris Artery Day-7 Post-Ligation A) Resting B) Maximally Dilated

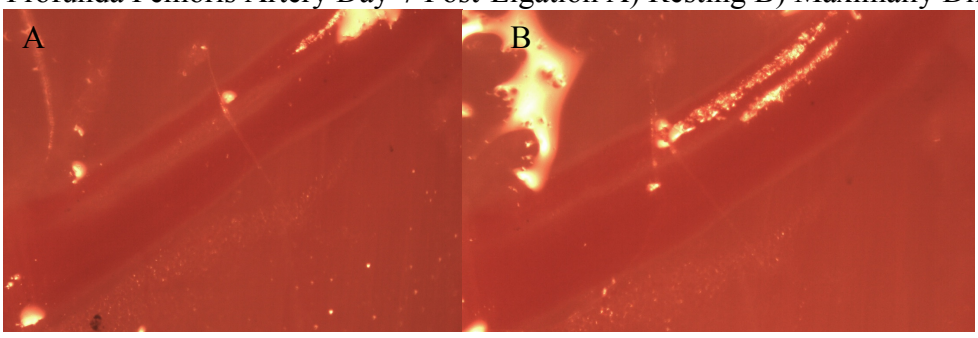

N=2 Profunda Femoris Artery Control A) Resting B) Maximally Dilated

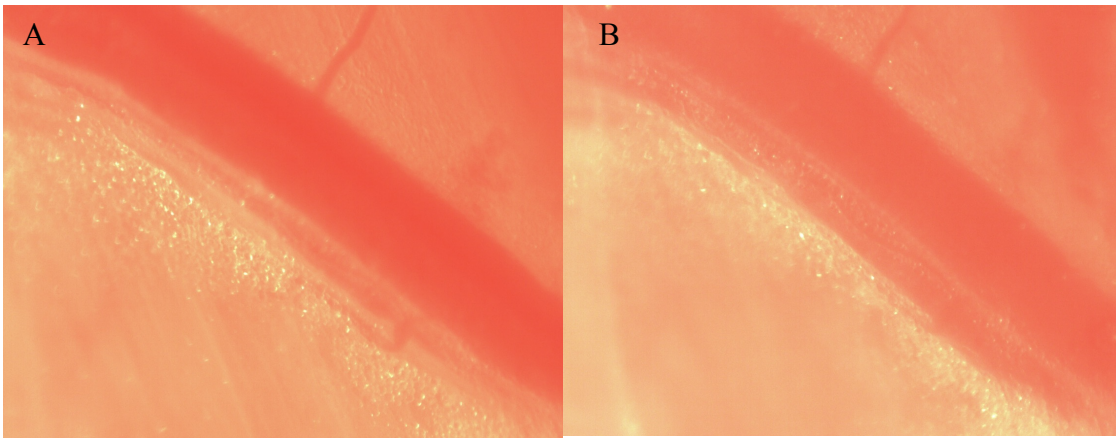

N=3 Profunda Femoris Artery Day-7 Post-Ligation A) Resting B) Maximally Dilated

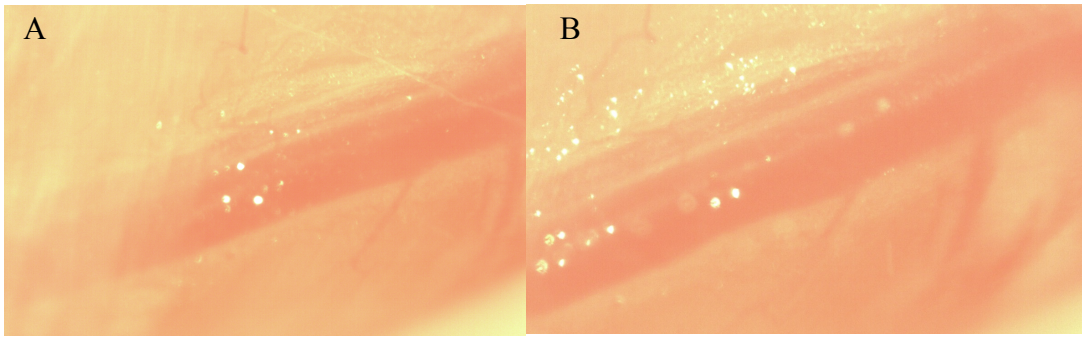

N=3 Profunda Femoris Artery Control A) Resting B) Maximally Dilated

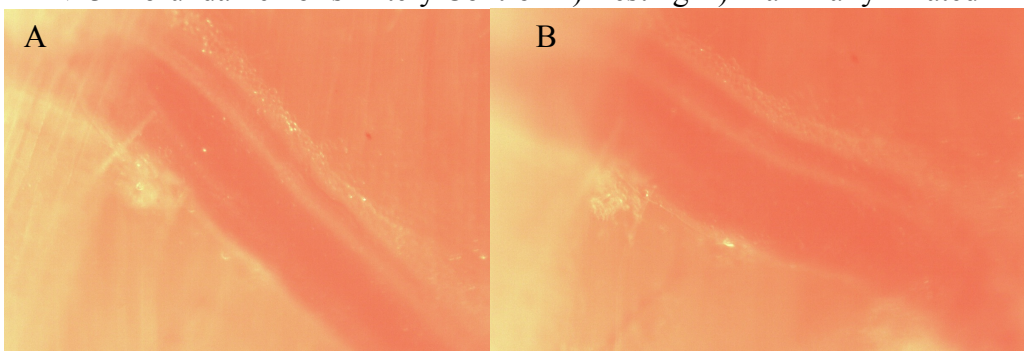

N=4 Profunda Femoris Artery Day-7 Post-Ligation A) Resting B) Maximally Dilated

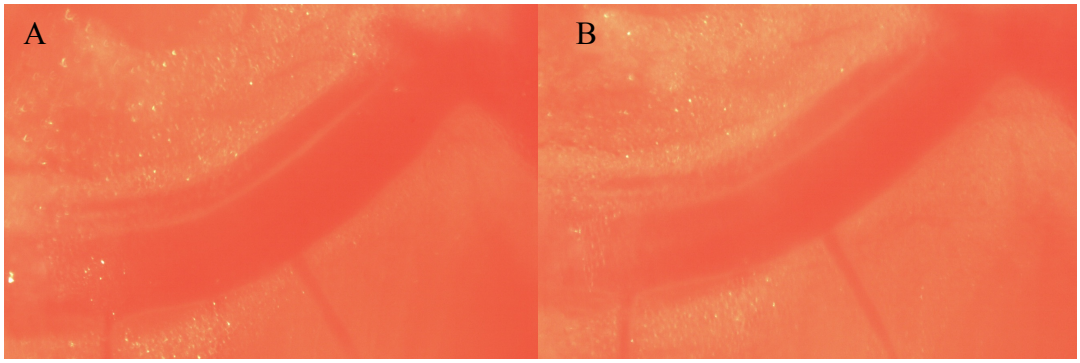

N=4 Profunda Femoris Artery Control A) Resting B) Maximally Dilated

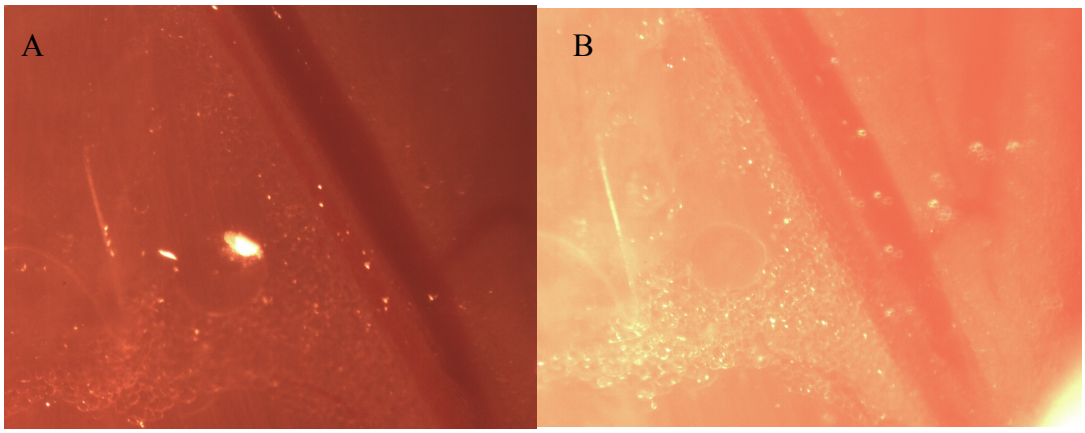

N=5 Profunda Femoris Artery Day-7 Post-Ligation A) Resting B) Maximally Dilated

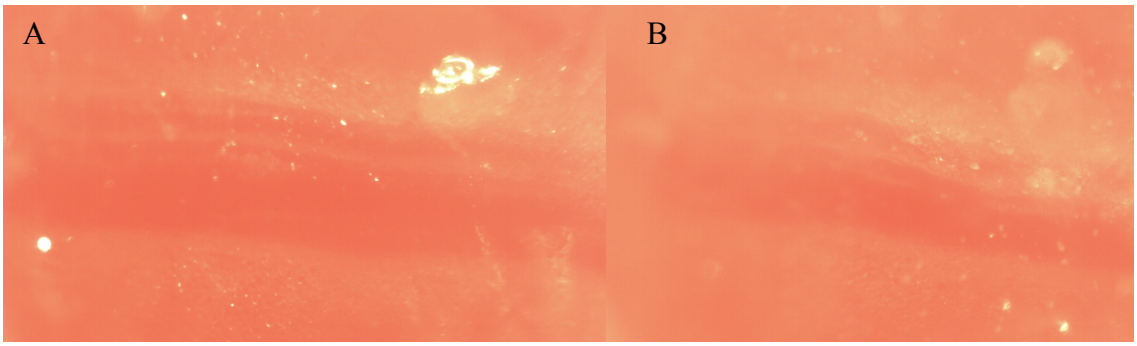

N=5 Profunda Femoris Artery Control A) Resting B) Maximally Dilated

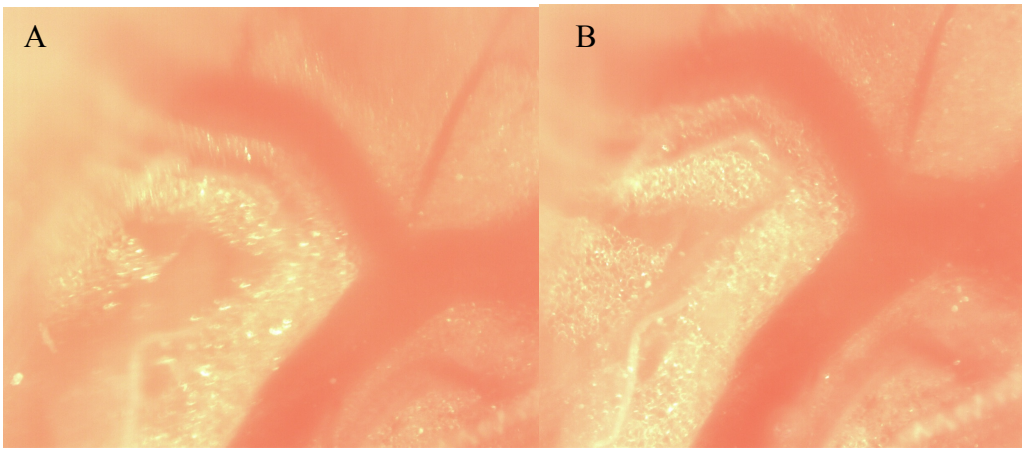

N=6 Profunda Femoris Artery Day-7 Post-Ligation A) Resting B) Maximally Dilated

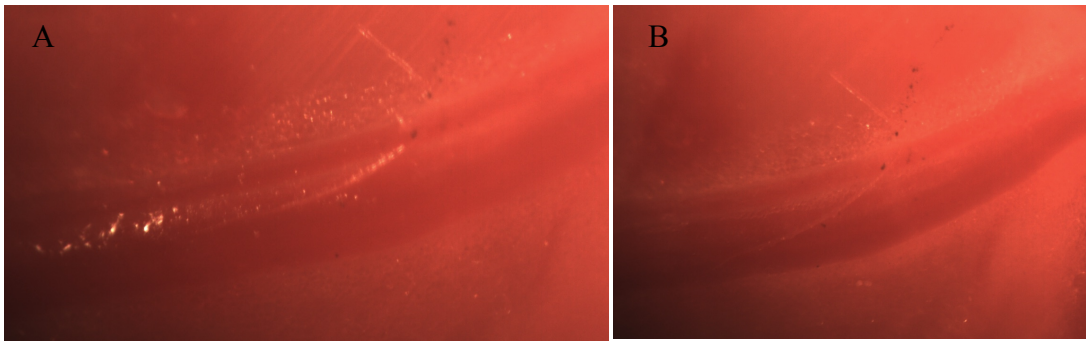

N=6 Profunda Femoris Artery Control A) Resting B) Maximally Dilated

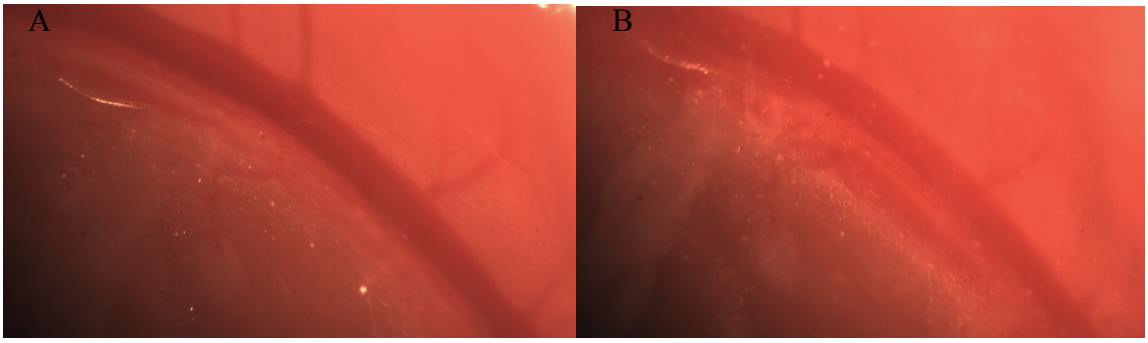

N=7 Profunda Femoris Artery Day-7 Post-Ligation A) Resting B) Maximally Dilated

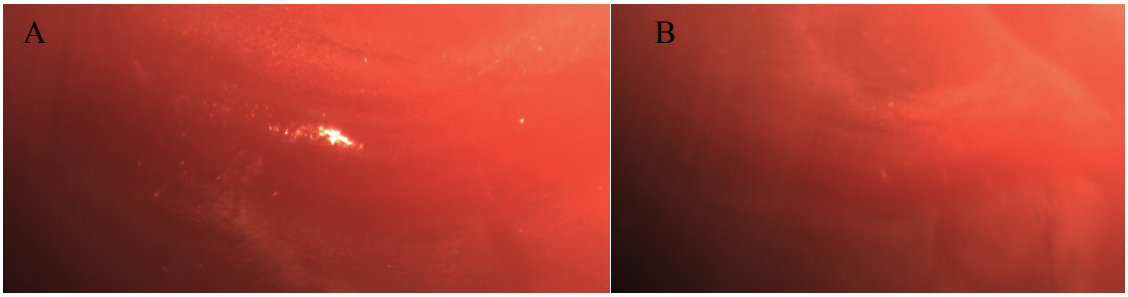

N=7 Profunda Femoris Artery Control A) Resting B) Maximally Dilated

Confocal Images (40x)

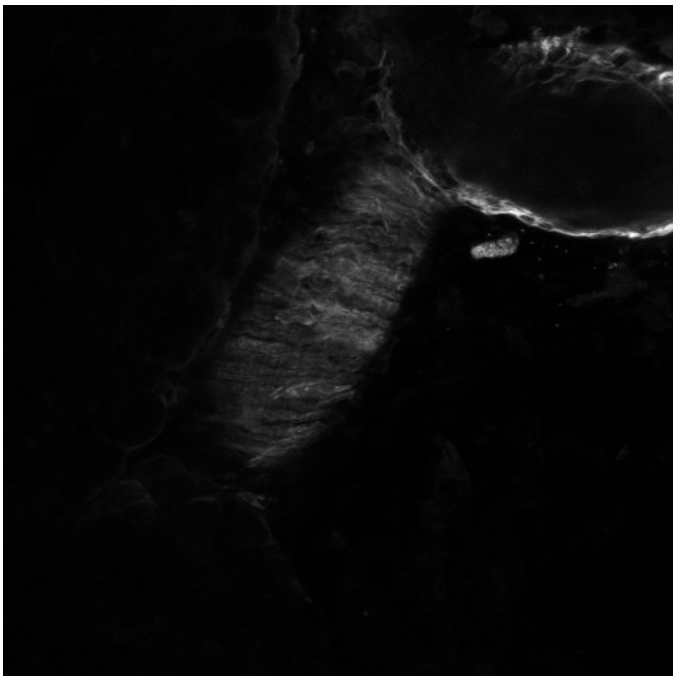

N=1 Profunda Femoris Artery Day-7

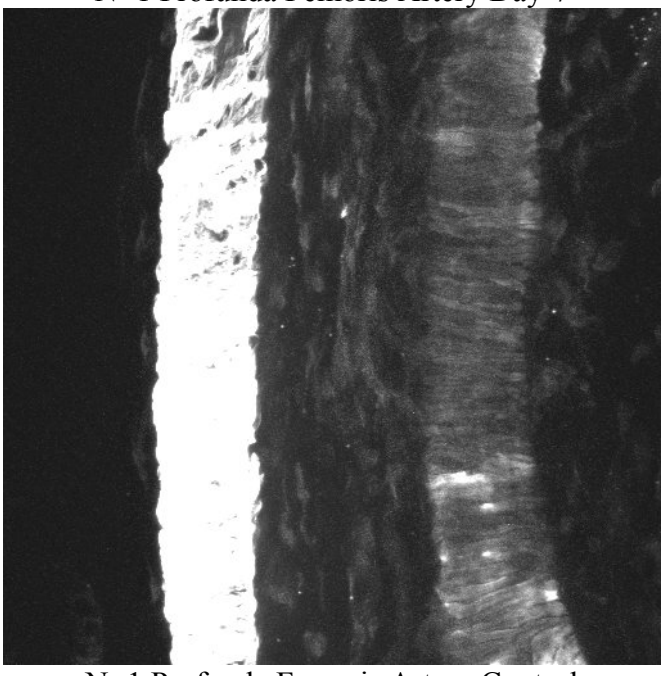

N=1 Profunda Femoris Artery Control

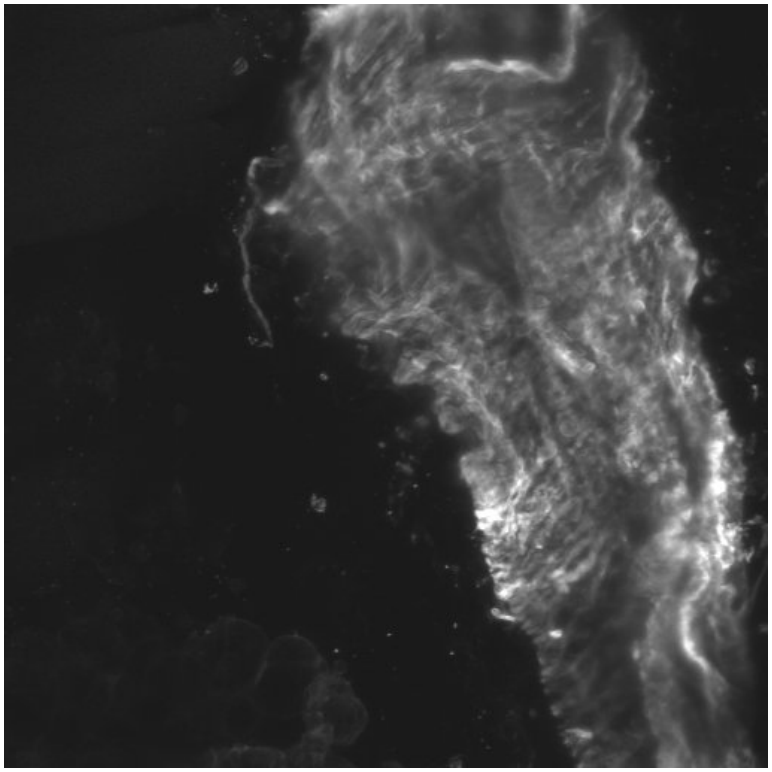

N=2 Profunda Femoris Artery Day-7

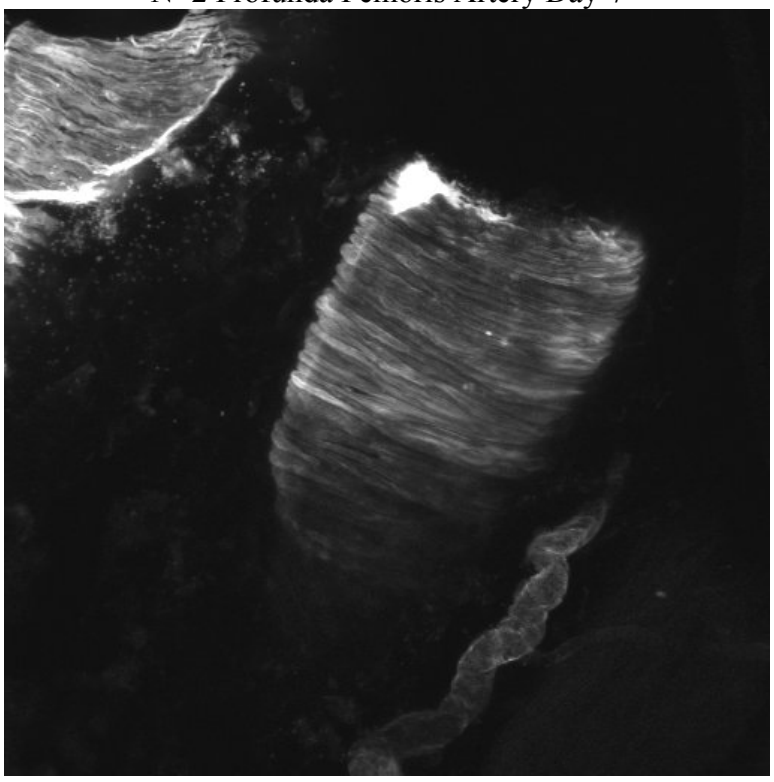

N=3 Profunda Femoris Artery Day-7

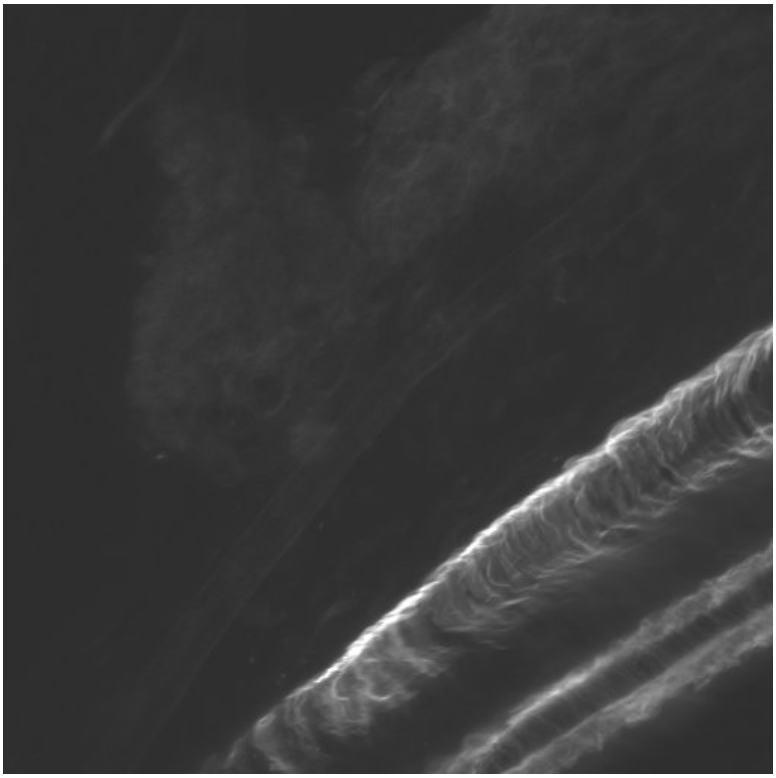

N=3 Profunda Femoris Artery Control

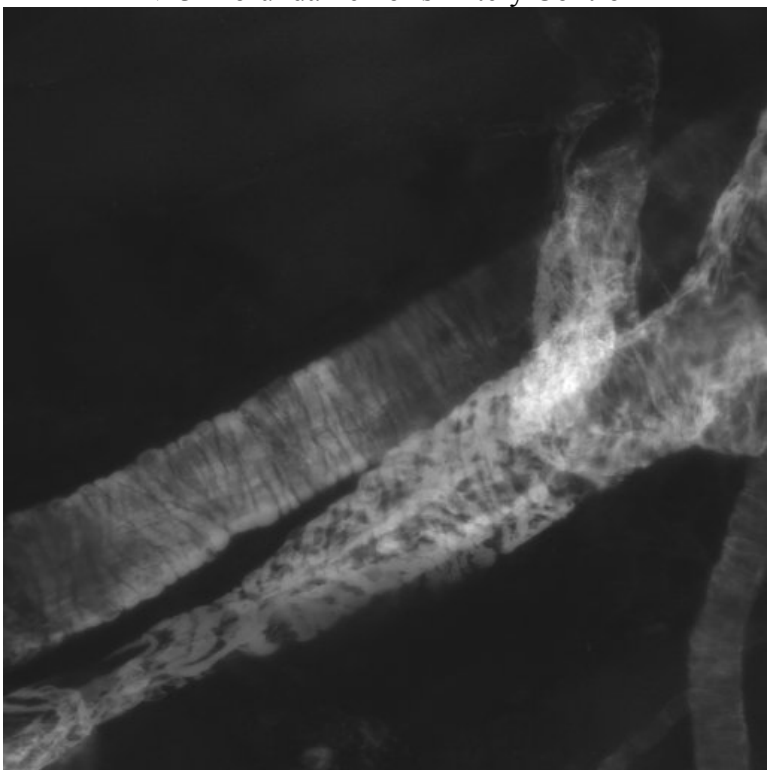

N=4 Profunda Femoris Artery Day-7

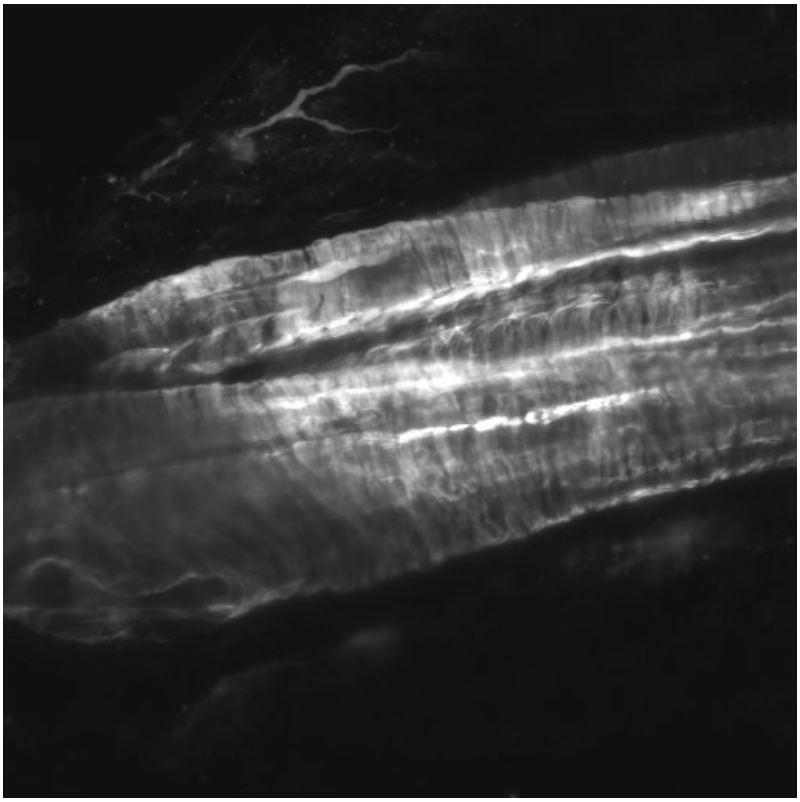

N=4 Profunda Femoris Artery Control

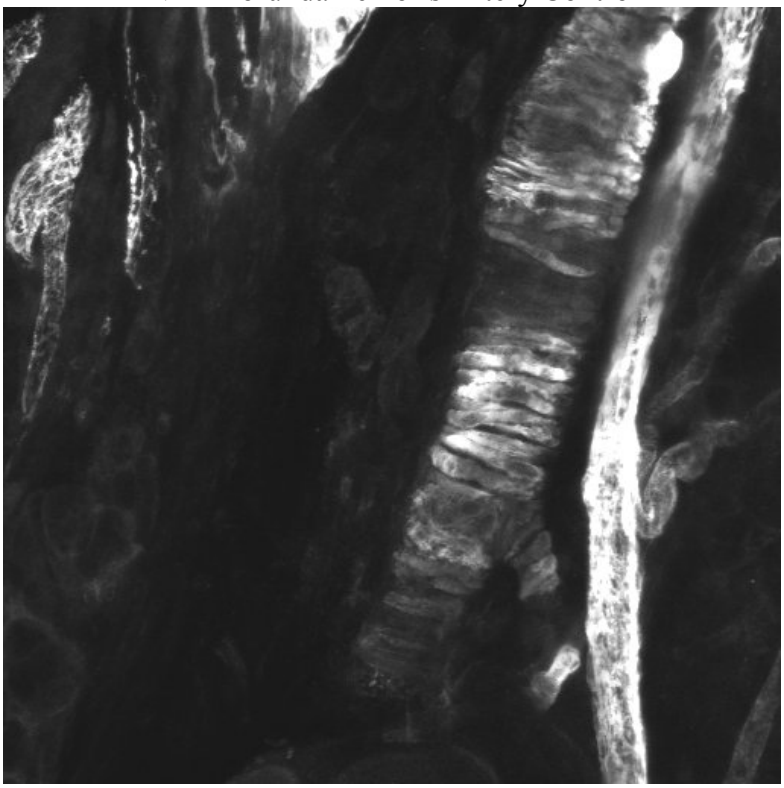

N=5 Profunda Femoris Artery Day-7

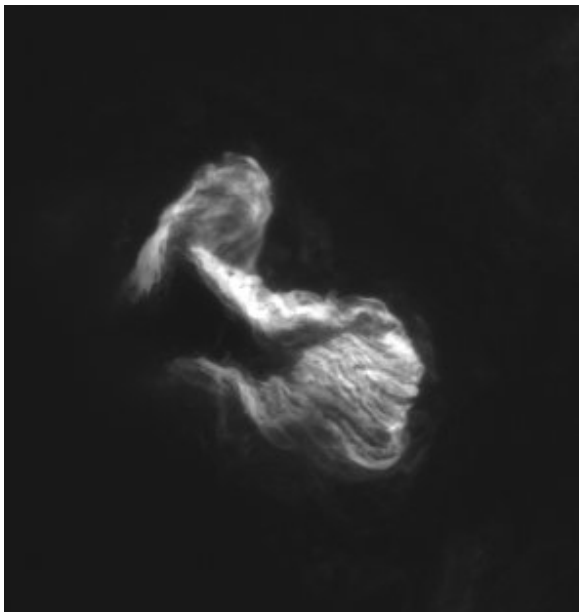

N=5 Profunda Femoris Artery Control

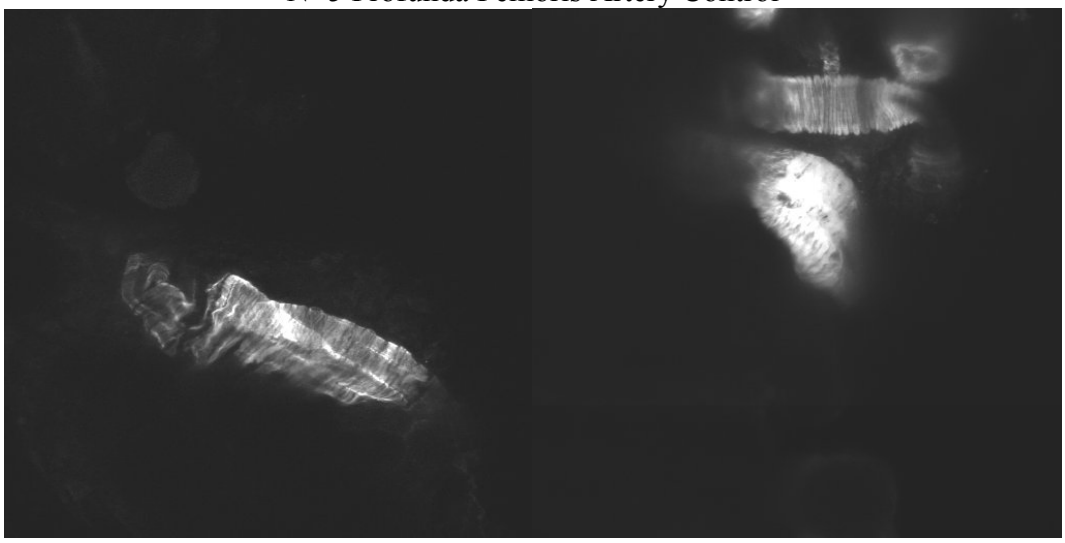

N=6 Profunda Femoris Artery Day-7

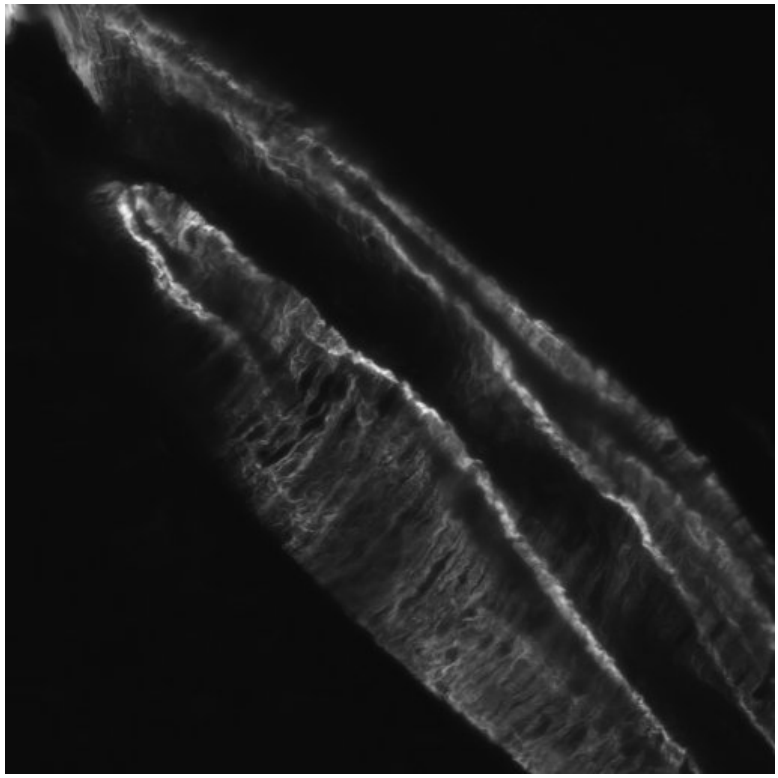

N=6 Profunda Femoris Artery Control

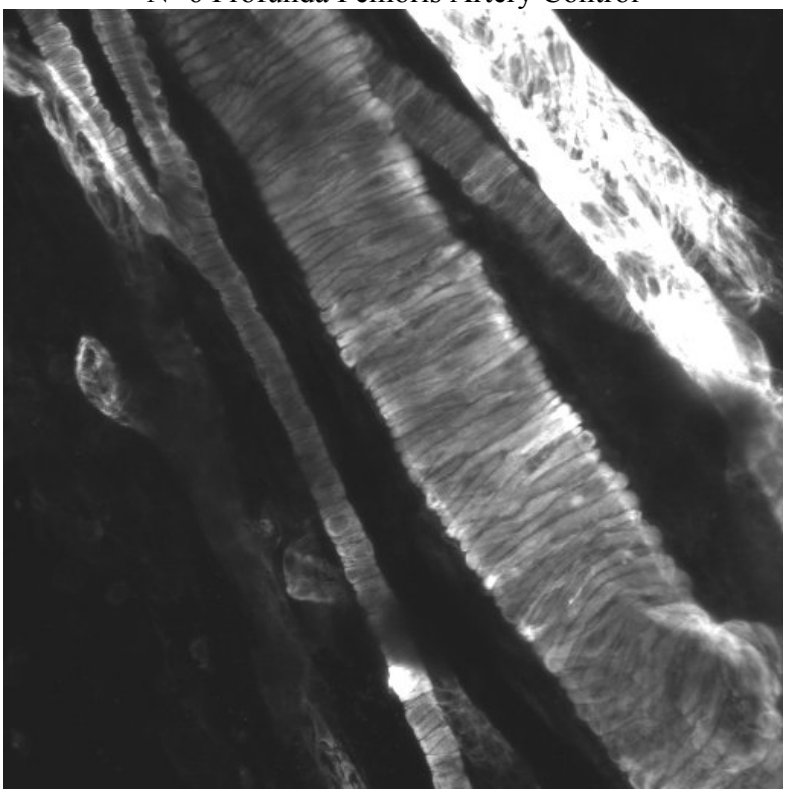

N=7 Profunda Femoris Artery Day-7

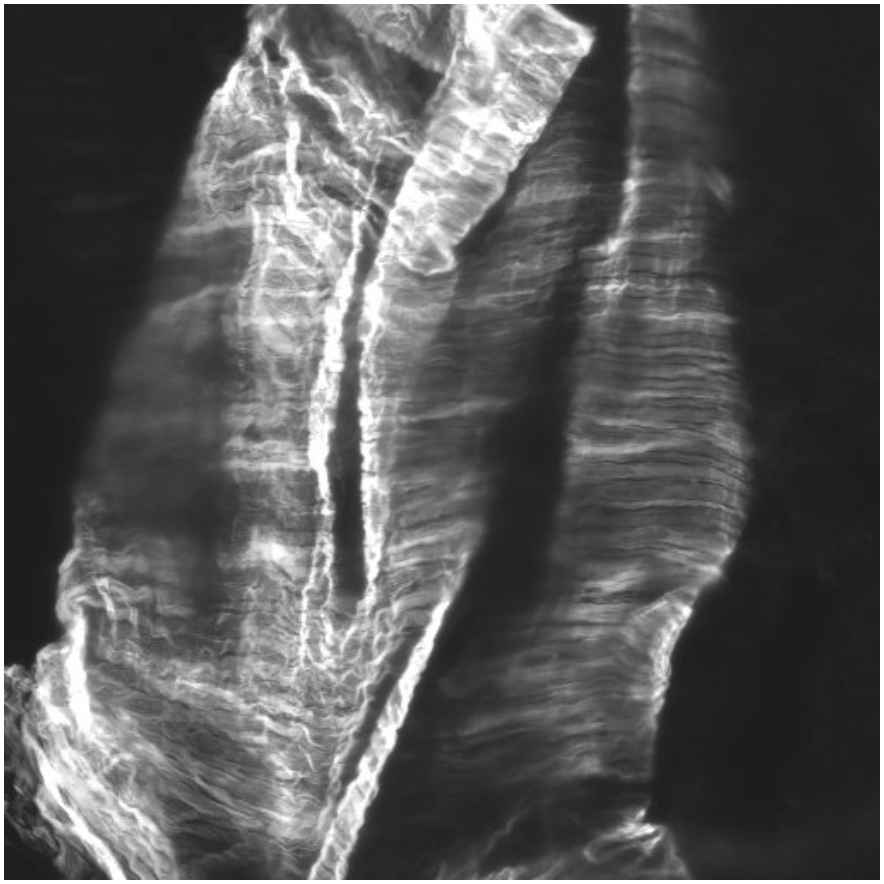

N=7 Profunda Femoris Artery Control

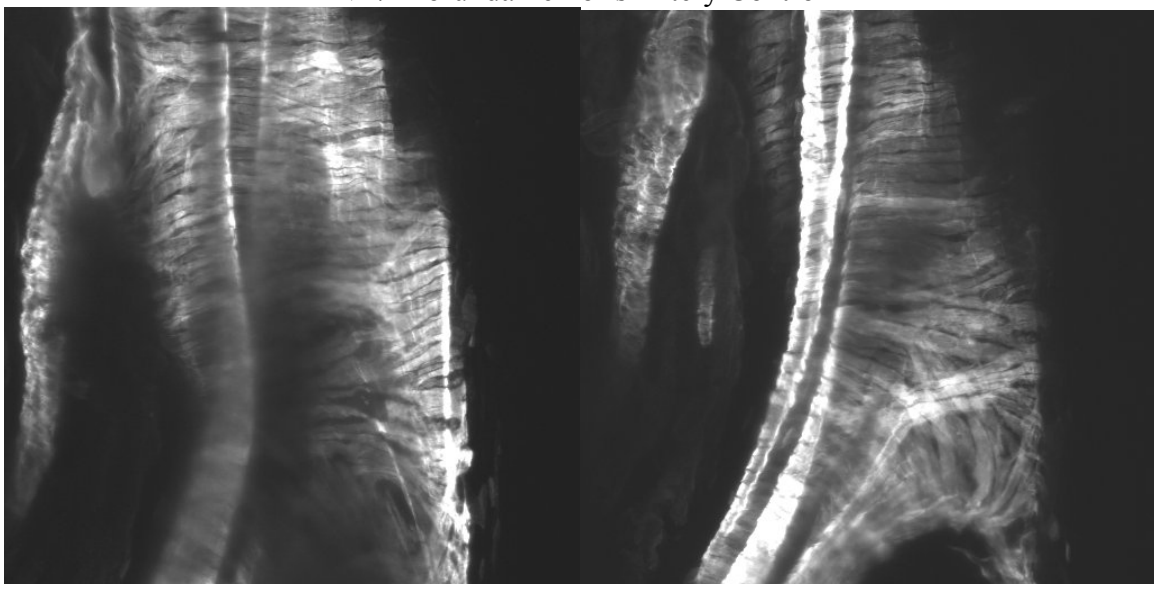

N=8 Profunda Femoris Artery Day-7

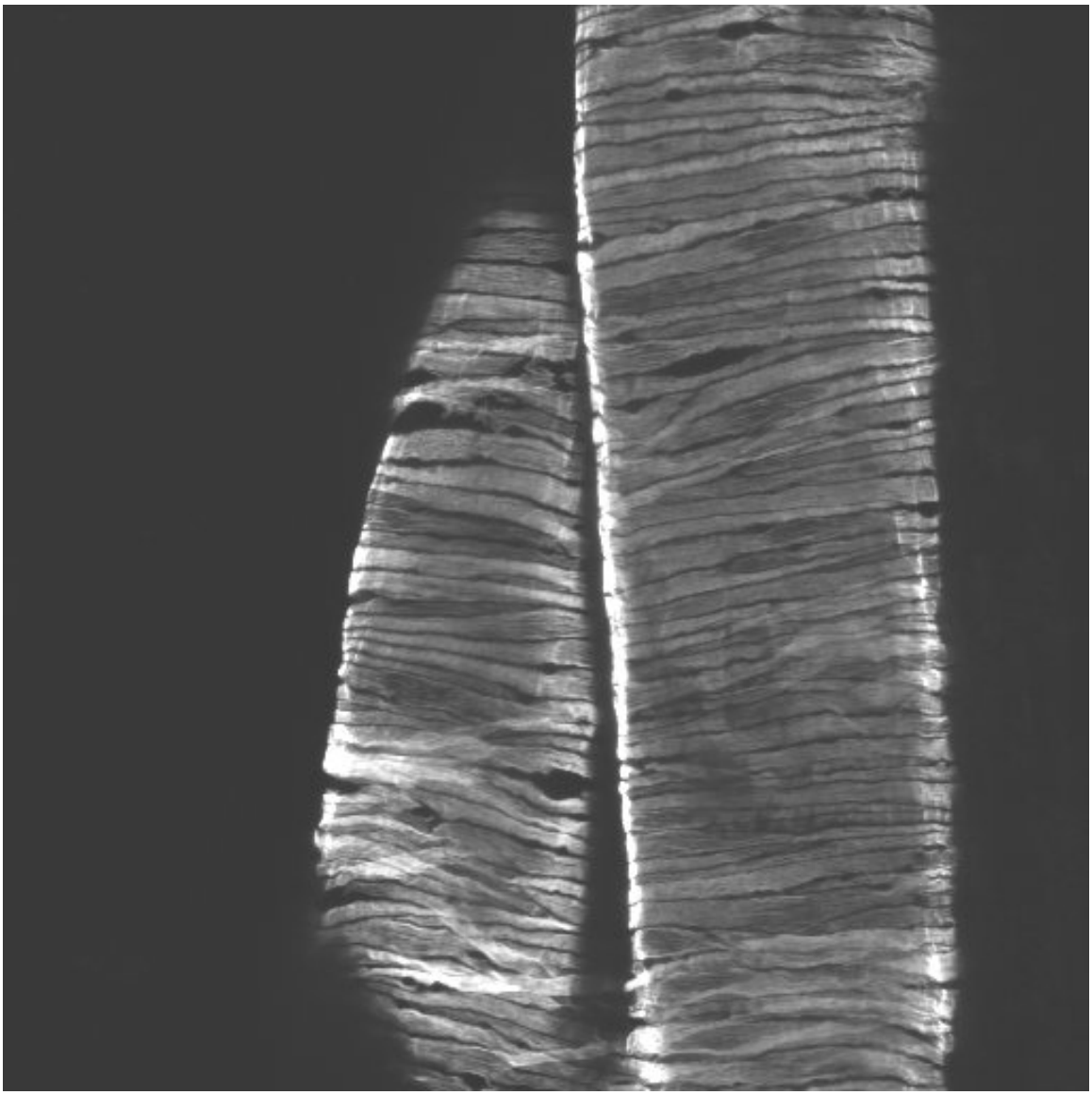

N=8 Profunda Femoris Artery Control